Search for $W' \to tb$ in proton-proton collisions at $\sqrt{s} = 8$ TeV

The CMS collaboration

E-mail: cms-publication-committee-chair@cern.ch

ABSTRACT: A search is performed for the production of a massive W' boson decaying to a top and a bottom quark. The data analysed correspond to an integrated luminosity of $19.7\,\mathrm{fb}^{-1}$ collected with the CMS detector at the LHC in proton-proton collisions at $\sqrt{s} = 8\,\mathrm{TeV}$. The hadronic decay products of the top quark with high Lorentz boost from the W' boson decay are detected as a single top flavoured jet. The use of jet substructure algorithms allows the top quark jet to be distinguished from standard model QCD background. Limits on the production cross section of a right-handed W' boson are obtained, together with constraints on the left-handed and right-handed couplings of the W' boson to quarks. The production of a right-handed W' boson with a mass below $2.02\,\mathrm{TeV}$ decaying to a hadronic final state is excluded at 95% confidence level. This mass limit increases to $2.15\,\mathrm{TeV}$ when both hadronic and leptonic decays are considered, and is the most stringent lower mass limit to date in the tb decay mode.

Contents

1 Introduction

Many extensions of the standard model (SM) predict new massive charged gauge bosons [1–3]. The W' boson, for example, is a heavy partner of the SM W gauge boson that could manifest itself in proton-proton collisions at the CERN LHC. Searches for a high-mass W' boson resonance have been performed at the Tevatron [4, 5] and the LHC [6–15] in the lepton, diboson, and diquark final states. We present a search based on the $\text{W}'^{+} \rightarrow \text{t}\bar{\text{b}}$ (and charge conjugate) decay. This decay channel is of particular interest because the SM backgrounds can be greatly reduced compared to those for W' decays to light quarks, and some models predict a stronger W' coupling to third generation quarks [16]. The hadronic decay channel (W' → tb → qqbb) is presented in detail, along with the combination with the already published leptonic channel (W' → tb → $\ell\nu$bb) [6]. The combination of these two channels leads to a significant increase in sensitivity.

The most general, lowest dimension effective Lagrangian that describes the interaction of the W' boson with quarks [17] can be written as:

$$\mathcal{L} = \frac{V_{q_i q_j}}{2\sqrt{2}} g_w \overline{q}_i \gamma_\mu \big(a^{R}_{q_i q_j}(1+\gamma^5) + a^{L}_{q_i q_j}(1-\gamma^5)\big) W' q_j + \text{h.c.,} \qquad (1.1)$$

where the parameters $a^{L}_{q_i q_j}$ and $a^{R}_{q_i q_j}$ represent the left-handed and right-handed couplings of the W' boson to quarks, g_W is the SM weak coupling constant, and $V_{q_i q_j}$ is the Cabibbo-Kobayashi-Maskawa matrix. For a SM-like W' boson, $a^{L}_{q_i q_j} = 1$, $a^{R}_{q_i q_j} = 0$.

Strict cross section upper limits have previously been placed in the case of low mass W' signals [5, 6]. At higher masses, specifically $M_{W'} \gtrsim 1.3\,\text{TeV}$, the top quark is highly energetic. Because of the Lorentz boost, the angular separation between the top quark decay products (W boson and b quark) is small. The final state particles resulting from the hadronization of the b quark and the decay of the W boson into light quarks usually overlap, resulting in a single jet with top flavour, the "top quark jet", or t jet. Dedicated methods, applied to resolve the substructure of this t jet, enable background processes to be strongly suppressed. We apply b jet identification algorithms (b tagging) to the b jet from the W' decay in order to further reduce the SM background.

We reconstruct the W' boson mass as the invariant mass of the top and bottom quarks (M_{tb}), and use the M_{tb} distribution to derive limits on the production cross section of the W' boson. We also obtain limits on the couplings of the W' boson to quarks, and present the W' production cross section limits obtained from a combination of hadronic and leptonic decay channels. The leptonic decay channel alone excludes a W' boson with a mass less than 2.05 TeV [6], which prior to this paper was the most restrictive limit obtained to date in the tb final state. The combination of the leptonic and hadronic channels makes it possible to extend this limit.

2 The CMS detector

The central feature of the CMS apparatus [18] is a superconducting solenoid of 6 m internal diameter, providing a magnetic field of 3.8 T. Within the field volume are a silicon pixel and strip tracker, a lead tungstate crystal electromagnetic calorimeter (ECAL), and a brass and scintillator hadron calorimeter (HCAL), each composed of a barrel and two endcap sections. Forward calorimeters extend the pseudorapidity coverage provided by the barrel and endcap detectors. Muons are measured in gas-ionization detectors embedded in the steel flux-return yoke outside the solenoid.

The silicon tracker detects charged particles within the pseudorapidity range $|\eta| < 2.5$. It consists of 1440 silicon pixel and 15 148 silicon strip detector modules and is located in the field of the superconducting solenoid. For non-isolated particles with $1 < p_T < 10\,\text{GeV}$ and $|\eta| < 1.4$, the track resolutions are typically 1.5% in p_T and 25–90 (45–150) μm in the transverse (longitudinal) impact parameter [19]. Non-isolated particle tracks are of particular importance to this analysis, as they are typically the constituents of jets, and are found within the detector barrel acceptance with an efficiency larger than 90%.

In the region $|\eta| < 1.74$, the HCAL towers have widths of 0.087 in pseudorapidity and 0.087 radians in azimuth (ϕ). In the η-ϕ plane, and for $|\eta| < 1.48$, the HCAL towers map on to 5×5 ECAL crystal arrays to form calorimeter towers projecting radially outwards from close to the nominal interaction point. At larger values of $|\eta|$, the size of the ECAL and HCAL towers increases and the matching ECAL arrays contain fewer crystals. Within each tower, the energy deposits in ECAL and HCAL towers are summed to define the calorimeter tower energies, which are subsequently used to provide the energies and directions of hadronic jets.

A more detailed description of the CMS detector, together with a definition of the coordinate system used and the relevant kinematic variables, can be found in ref. [18].

3   Event reconstruction

The particle-flow (PF) event algorithm [20, 21] reconstructs and identifies each individual particle with an optimized combination of information from the various elements of the CMS detector. The energy of photons is directly obtained from the ECAL measurement, corrected for zero-suppression effects. The energy of electrons is determined from a combination of the electron momentum at the primary interaction vertex as determined by the tracker, the energy of the corresponding ECAL cluster, and the energy sum of all bremsstrahlung photons spatially compatible with originating from the electron track. The momentum of muons is obtained from the curvature of the corresponding track as determined by the tracker and muon system. The energy of charged hadrons is determined from a combination of their momentum measured in the tracker and the matching ECAL and HCAL energy deposits, corrected for zero-suppression effects and for the response function of the calorimeters to hadronic showers. Finally, the energy of neutral hadrons is obtained from the corresponding corrected ECAL and HCAL energies.

Jets are reconstructed using the Cambridge-Aachen (CA) [22, 23] algorithm with a distance parameter of 0.8 (CA8 jets) as implemented by FastJet 3.0.4 [24, 25] to cluster PF candidates into jets. This algorithm clusters constituents (the reconstructed PF candidates in each event) to form jets based only on the angular distance between them. The CA algorithm has been shown to have higher efficiency for distinguishing jet substructure [26] than competing jet clustering algorithms.

Jet momentum is determined as the vector sum of all particle momenta in the jet, and is found in the simulation to be equal to the true momentum at hadron level within 5% to 10% over the full p_T spectrum and detector acceptance.

The jet energy resolution amounts typically to 15% at 10 GeV, 8% at 100 GeV, and 4% at 1 TeV, to be compared to about 40%, 12%, and 5% obtained jet clustering is based on calorimeter information only rather than on PF candidates.

The jet energy in simulation is corrected using measurements derived from data. The jet energy corrections for the CA jets are derived from the anti-k_T (AK) jet clustering algorithm [27] with a distance parameter value of 0.7. The AK jet energy corrections have been shown to be applicable to CA jets [28]. The uncertainty associated with this procedure is noted in section 6.1.

We use the charged hadron subtraction method [29] to remove charged hadrons that originate from a non-leading vertex prior to the application of the jet clustering algorithm, where the leading vertex is defined as the vertex with the largest sum of p_{T}^2. After this procedure, the neutral component of pileup (inelastic proton-proton pair interactions in the same bunch crossing) is subtracted using an area based method [30].

3.1 Signal modeling

The signal samples are generated at leading order with the CompHEP [31] package and then scaled to next-to-leading order using a factor of 1.2 [17]. We generate signal samples using three coupling hypotheses (see eq. (1.1)):

- $\mathbf{W'_R}$ — purely right-handed W' boson where $a_{\mathrm{q}_i\mathrm{q}_j}^{\mathrm{L}}=0$ and $a_{\mathrm{q}_i\mathrm{q}_j}^{\mathrm{R}}=1$;

- $\mathbf{W'_L}$ — purely left-handed W' boson where $a_{\mathrm{q}_i\mathrm{q}_j}^{\mathrm{L}}=1$ and $a_{\mathrm{q}_i\mathrm{q}_j}^{\mathrm{R}}=0$;

- $\mathbf{W'_{LR}}$ — mixed-coupling W' boson where $a_{\mathrm{q}_i\mathrm{q}_j}^{\mathrm{L}}=1$ and $a_{\mathrm{q}_i\mathrm{q}_j}^{\mathrm{R}}=1$.

The $\mathrm{W'_R}$ width varies from 44 to 91 GeV for the mass range considered in this analysis. The generation of the left-handed and mixed-coupling samples takes into account the interference with the SM s-channel single top quark production.

3.2 Combined CMS t-tagging algorithm

When the W boson decays to hadrons, the top quark can be detected as three jets. The high boost of the top quark from a W' boson decay causes the three jets to merge into one large jet with a distinct substructure. The CMS t-tagging algorithm [32] discriminates signal from background by using this characteristic substructure. The algorithm reclusters the CA jet until it finds anywhere from 1 to 4 subjets In this process, particles with low p_{T} or at a large angular distance from the jet centre are omitted. The t-tagging algorithm is based on the following selection:

- **Jet mass $140 < M_{\mathbf{jet}} < 250\,\mathbf{GeV}$** — The mass of the CA jet is required to be consistent with the top quark mass.

- **Number of subjets $N_{\mathbf{subjets}} > 2$** — The number of subjets found by the algorithm must be at least 3.

- **Minimum pairwise mass $M_{\mathbf{min}} > 50\,\mathbf{GeV}$** — The three highest p_{T} subjets are taken pairwise, and the pair with the lowest invariant mass is calculated (M_{min}). The value of M_{min} is required to be greater than 50 GeV for consistency with the W boson mass.

In addition to these requirements, the N-subjettiness algorithm is used for t-jet identification [33]. This algorithm defines the τ_N variables, which describe the consistency between the jet energy and the number of assumed subjets, N:

$$\tau_N = \frac{1}{d} \sum_i p_{\mathrm{T}_i} \min\{\Delta R_{1,i}, \Delta R_{2,i}, \ldots, \Delta R_{N,i}\}, \tag{3.1}$$

where $\Delta R_{\mathrm{J},i}$ is the angular distance ($\Delta R = \sqrt{(\Delta\eta)^2 + (\Delta\phi)^2}$) measured between the subjet candidate (J) axis and a specific constituent particle (i), and d is the normalization factor:

$$d = \sum_i p_{\mathrm{T}_i} R, \tag{3.2}$$

where R is the characteristic distance parameter used by the jet clustering algorithm. A jet with energy consistent with N subjets will typically have a low τ_N variable. A t jet should be more consistent with three subjets than two (when compared to jets originating from a gluon or a light quark), therefore the ratio of τ_3 and τ_2 allows top jets to be distinguished from multijet events from QCD processes (labeled in the following as QCD background). We select events with $\tau_3/\tau_2 < 0.55$.

We apply the combined secondary vertex (CSV) b-tagging algorithm to all of the subjets found by the t-tagging algorithm. We require the maximum CSV discriminator value to pass CSV b tagging at the medium operating point ($\mathrm{SJ_{CSVMAX}} \geq 0.679$) [34]. The CMS t tagger with the addition of N-subjettiness and subjet b tagging is referred to as the combined CMS t tagger.

Substructure variables in the signal region exhibit known differences between data and simulation that affect the t-tagging efficiency. We derive a scale factor that is the ratio of the t-tagging efficiency measured in data to simulation [32], using hadronic top quark decays from a control region that consists of an almost pure sample of semileptonic $t\bar{t}$ events. This ratio, which is measured to be 1.04 ± 0.13, is applied as a correction factor to the signal samples that are used in this analysis.

3.3 Identification of b jets

To identify the b quark daughter of the W$'$ boson, we start with the b-candidate jet, which is the highest p_{T} jet that is hemispherically separated from the top-tagged jet. We apply the CSV algorithm used to identify b jets to this b-candidate jet. The medium operating point is used, which has a light-flavour jet misidentification probability of 1% for an efficiency around 70%. A scale factor is applied to correct for differences in b-tagging efficiency between data and simulation [34]. The uncertainties in this scale factor are described in section 6.1. Backgrounds from SM $t\bar{t}$ production are reduced by requiring the invariant mass of the b-candidate CA jet to be below 70 GeV.

3.4 Reconstruction of W$'$ mass

We select candidate W$' \to$ tb events by using the following criteria, which are applied to the two leading jets:

- One jet with $p_{\mathrm{T}} > 450\,\mathrm{GeV}$ identified with the combined CMS t-tagging algorithm;

- One jet with $p_{\mathrm{T}} > 370\,\mathrm{GeV}$ with a CSV b tag at the medium operating point and mass $<70\,\mathrm{GeV}$;

- The two jets are in opposite hemispheres ($|\Delta\phi| > \pi/2$);

- The difference in rapidity between the two jets ($|\Delta y|$) is less than 1.6.

Selection	Data	QCD	$t\bar{t}$	ST_s	$M_{W'_R}$ 1.90 TeV	$M_{W'_R}$ 2.10 TeV	$M_{W'_L}$ 1.90 TeV	$M_{W'_L}$ 2.10 TeV
2 jets	13854873	—	12190 ± 27	283 ± 8.6	806 ± 1	401 ± 0.7	796 ± 2	430 ± 2
p_T	4305244	—	4720 ± 18	130 ± 6.5	739 ± 1	372 ± 0.7	703 ± 2	364 ± 2
$|\Delta y|$	3376771	—	4220 ± 17	121 ± 6.3	553 ± 1	268 ± 0.6	531 ± 2	268 ± 1
M_t	992949	—	3220 ± 14	64 ± 4.5	429 ± 1	209 ± 0.5	414 ± 2	205 ± 1
$N_{subjets}$	557489	—	2740 ± 13	48 ± 3.9	340 ± 0.9	163 ± 0.5	312 ± 2	152 ± 1
M_{min}	318520	—	2510 ± 13	42 ± 3.7	304 ± 0.9	143 ± 0.4	274 ± 2	130 ± 0.9
SJ_{CSVMAX}	50642	—	1690 ± 10	23 ± 2.6	170 ± 0.6	76 ± 0.3	138 ± 1	63 ± 0.6
τ_3/τ_2	7200	—	1024 ± 8	11 ± 1.8	88 ± 0.5	38 ± 0.2	58 ± 0.7	27 ± 0.4
M_b	4463	—	178 ± 4	8 ± 1.6	68 ± 0.4	29 ± 0.2	44 ± 0.6	20 ± 0.3
CSV	277	248 ± 4	37 ± 1	2 ± 0.71	16 ± 0.2	6 ± 0.1	10 ± 0.3	4 ± 0.2

Table 1. Numbers of observed and expected events at successive stages of the event selection. The expected numbers are scaled to an integrated luminosity of $19.7\,\mathrm{fb}^{-1}$. Statistical uncertainties in the event yields are quoted. The QCD background contribution is only reported for the final selection. The first row implies a $150\,\mathrm{GeV}$ p_T selection on the jets, the trigger selection, and the requirement that the two leading jets be in opposite hemispheres. The row labeled "p_T" represents the transverse momentum requirements placed on the two leading jets. The signal events, shown for several values of the W$'$ boson mass, are normalized to the theoretical cross section. The s-channel single top contribution (ST_s) is given as well as it is used when deriving the shape of the signal distribution when calculating the generalized coupling limits.

The number of events after each successive selection remaining in data, SM $t\bar{t}$ production, s-channel single top, and right-handed W$'$ boson signal simulations is shown in table 1.

4 Event samples

The data used for this analysis correspond to an integrated luminosity of $19.7\,\mathrm{fb}^{-1}$ of pp collisions provided by the LHC at a centre-of-mass energy of $8\,\mathrm{TeV}$. We select events online using a trigger algorithm that requires the scalar p_T sum of reconstructed jets in the detector to be $>750\,\mathrm{GeV}$. The trigger is nearly 100% efficient for events selected in the offline analysis. The small trigger inefficiency is measured from data and applied to the simulated events.

5 Background modeling

The primary sources of background are SM QCD multijet and $t\bar{t}$ production. These backgrounds dominate because of QCD background events after selecting an all-jet final state is selected and the large contribution from $t\bar{t}$ production that remains after t-jet discrimination criteria are applied.

The principal background in this analysis is QCD multijet production, and is estimated using a data-driven technique to extract both the shape and the normalization. The average b-tagging rate, measured from events with an enhanced QCD multijet component and a negligible signal contamination component, is used to estimate the QCD multijet

contribution in the signal region. We account for the background contribution from SM $t\bar{t}$ production when measuring the b-tagging rate. In addition to the region used to extract the average b-tagging rate, we define two test regions to check the QCD background prediction, both of which have small $t\bar{t}$ background and possible signal contamination.

The shape of the M_{tb} distribution for $t\bar{t}$ production is estimated from Monte Carlo (MC) simulation, and the yield is measured from data using a control sample enriched in $t\bar{t}$ events.

5.1 QCD background estimate

A control sample is obtained by inverting the N_{subjets} selection criteria used to identify t jets:

$$140 < M_{\mathrm{jet}} < 250\,\mathrm{GeV};\tag{5.1}$$

$$N_{\mathrm{subjets}} \leq 2;\tag{5.2}$$

$$\mathrm{SJ}_{\mathrm{CSVMAX}} \geq 0.679.\tag{5.3}$$

We apply the b tagging criteria to the b-candidate jet in the event to measure the average b-tagging rate for QCD jets. We assume that this rate is the same for QCD jets in the signal region. We include the subjet CSV discriminant in this control sample in order to ensure similar parton flavour distributions in the signal and control regions. Because of the similar parton flavour distributions, and the fact that this region has a low $t\bar{t}$ and signal contamination component, this control sample is an ideal selection to extract the average b-tagging rate. The average b-tagging rate is parameterized as a function of the p_{T} of the b-candidate jets (which pass all requirements except the b tag) in three $|\eta|$ regions:

- Low $(0.0 < |\eta| \leq 0.5)$;

- Transition $(0.5 < |\eta| \leq 1.15)$;

- High $(1.15 < |\eta| \leq 2.4)$.

Events in the signal region that do not have b tagging applied are then weighted by this average b-tagging rate to estimate the QCD background contribution in the final selection. Events in the signal region before b tagging is applied are largely from QCD background, but the small $t\bar{t}$ background component (less than 1%) is subtracted when deriving the QCD background contribution to avoid double counting.

We use a bifurcated polynomial to fit the average b-tagging rate in each of these $|\eta|$ ranges. This fitting function, which provides a satisfactory description of the data, is defined as follows:

$$f(x) = \begin{cases} p_0 + p_1 x + p_2 (x-a)^2, & \text{if } x < a \\ p_0 + p_1 x + p_3 (x-a)^2, & \text{if } x \geq a \end{cases}\tag{5.4}$$

Here, the parameters p_0 to p_3 are the polynomial coefficients, and x is the p_{T} of the b-candidate jet. The parameter a is the bifurcation point, and is optimized for each region
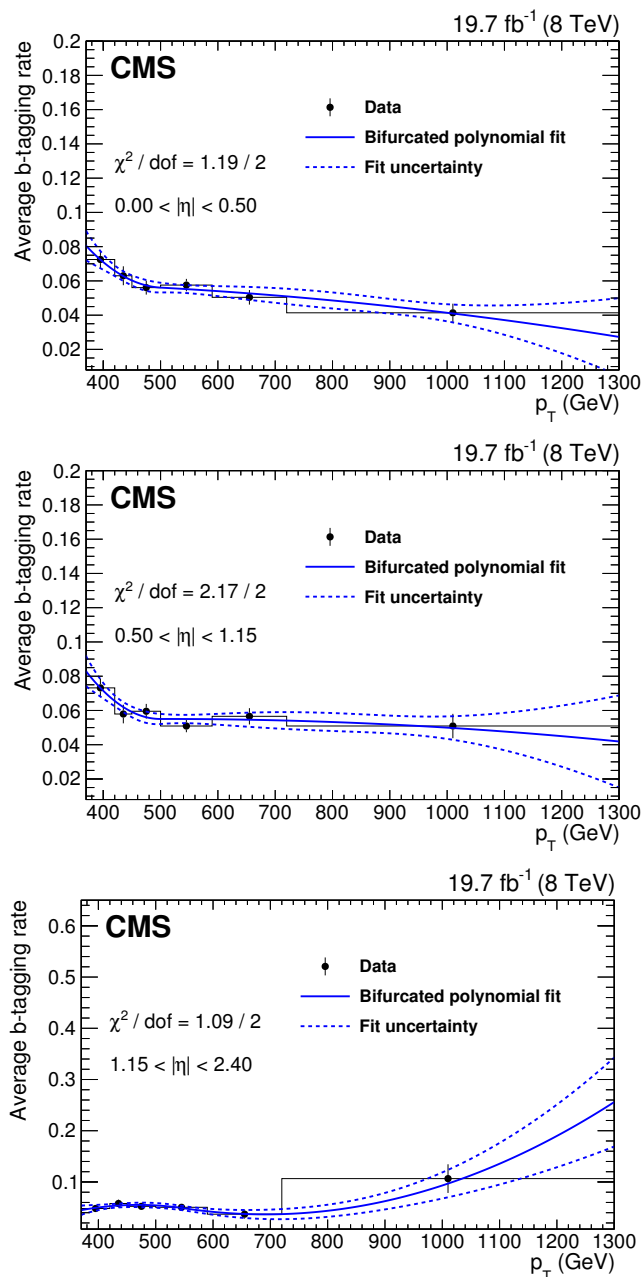
Figure 1. The average b-tagging rate for QCD jets parameterized as a function of the p_{T} of the b-jet candidate from the low (top), transition (middle), and high (bottom) $|\eta|$ regions. The measured average b-tagging rate is represented by the data points, the polynomial fit is shown as a solid line, and the propagated uncertainties from the fit are shown as the dashed lines. The horizontal lines on the data points indicate the bin widths.

in $|\eta|$. It is chosen to be 500, 500, and 550 GeV for the low, transition, and high $|\eta|$ regions, respectively. The parameterization of the average b-tagging rate helps to constrain the known p_{T} and $|\eta|$ kinematic correlation inherent in b tagging, which is due to detector geometry and tracking resolution.

The uncertainty in the average b-tagging rate is extracted using the full covariance matrix obtained from the output of the fitting algorithm. Additionally, we assign a systematic uncertainty to cover the choice of the fit function (see section 6.1) based on several alternative functional forms (such as second degree polynomial or exponential functions). Figure 1 shows the measured average b-tagging rate and associated uncertainty bands.

5.2 The $t\bar{t}$ background estimate

We obtain the normalization of the background contribution from SM $t\bar{t}$ production using a control sample in data. A sideband region is defined (CR3) by inverting the b-candidate mass requirement (see section 3.3) in the signal region. This region has an enhanced fraction of $t\bar{t}$ events and is statistically independent from all other sidebands in the analysis.

We compare the sum of the QCD background estimate from data and the SM $t\bar{t}$ contribution obtained from MC simulation to the observed yield in data. The $t\bar{t}$ and single top quark production samples used in this analysis are generated using the POWHEG [35–37] 1.0 event generator and are normalized to the SM expectation using next-to-next-to leading-order cross sections [38, 39].

For the QCD background determination in this sideband region, we use the procedure outlined in section 5.1. However, we invert the b-candidate mass requirement when extracting the average b-tagging rate in order to account for potential correlations between the b-candidate mass and the b-tagging rate.

We perform a binned maximum likelihood fit to the invariant mass distribution of the b-candidate jets, using the shape of the $t\bar{t}$ background MC prediction as one template, and the QCD background prediction from data as the other. The normalization of the QCD background template is allowed to vary within its systematic uncertainty envelope, whereas the normalization of the $t\bar{t}$ template is left unconstrained. The result of the fit is shown in figure 2.

The contamination from $t\bar{t}$ events must be taken into account when obtaining the QCD background template in this sideband from data. The fit described above independently varies the QCD and $t\bar{t}$ templates, however the component of the QCD background from $t\bar{t}$ events introduces a small anticorrelation between the two templates. We account for this by first fitting the QCD background before the $t\bar{t}$ component is subtracted and correcting the resulting $t\bar{t}$ normalization by the factor $1+C/S$, where C/S is the ratio of the nominal number of $t\bar{t}$ events in the control region (C) to that in the signal region (S). After applying this correction, the $t\bar{t}$ normalization obtained from the fit is independent of the fraction subtracted from the QCD background template. Following this procedure we find that the SM $t\bar{t}$ production rate in the signal region must be scaled by a factor of 1.23 ± 0.24.

In order to correct for known differences in the top quark p_{T} spectrum between data and MC simulation of SM $t\bar{t}$ production [40], we reweight the MC events using the generator level p_{T} of the top quark and top anti-quark. Although this procedure was not designed for the kinematic range in our analysis, we still use it as the change to the normalization of the $t\bar{t}$ background template is consistent with our measurement of this extra normalization factor.
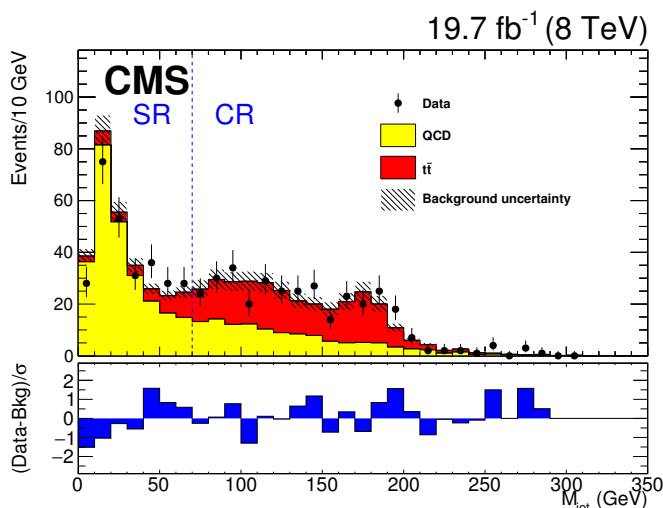
Figure 2. Distribution of the mass of the b-jet candidate after the template fit to constrain the QCD multijet and $t\bar{t}$ backgrounds has been applied. A control region with inverted selection criteria on the mass of the b-jet candidate is used for the fit, and is shown as the area to the right of the vertical dashed line. The hatched region represents the background uncertainty, obtained by adding the QCD multijet uncertainty and the uncertainty on the $t\bar{t}$ normalization from the output of the fit in quadrature. The bottom plot shows the pull ((data-background)/σ) between the data and the background estimate distributions.

5.3 Control region closure test

To investigate the applicability of the QCD background estimation in data, we apply the average b-tagging rate to control regions of the t-tagging selection defined in section 3.2. First, we define a control region with inverted minimum pairwise mass and N-subjettiness selections (CR1). This region is orthogonal to both the signal region and the control region that is used for the determination of the average b-tagging rate. The selection also has a very low yield of $t\bar{t}$ production, which allows for a precise measurement of the QCD background contribution. The average b-tagging rate used for this closure test is extracted from the same control region as the signal region, and is applied to events that are not b tagged. This test shows good agreement as shown in figure 3 (top). Additionally, we define a control region with an inverted subjet b-tagging selection (CR2). This test also shows good agreement as seen in figure 3 (bottom).

These control regions have low signal contamination. For the 1.90 TeV W'_R sample, the signal contamination is less than 1%. These control regions are summarized in table 2.

6 Results

After constraining the SM $t\bar{t}$ normalization using a particular control region (see section 5.2), and investigating the agreement of the data and the QCD background estimate in two additional control regions (see section 5.3), the background estimate is used to predict the data distribution in the signal region, in the absence of a W' boson contribution. The results are shown in figure 4. Good agreement between data and expectation from SM processes are observed, with no signs of a new physics signal.
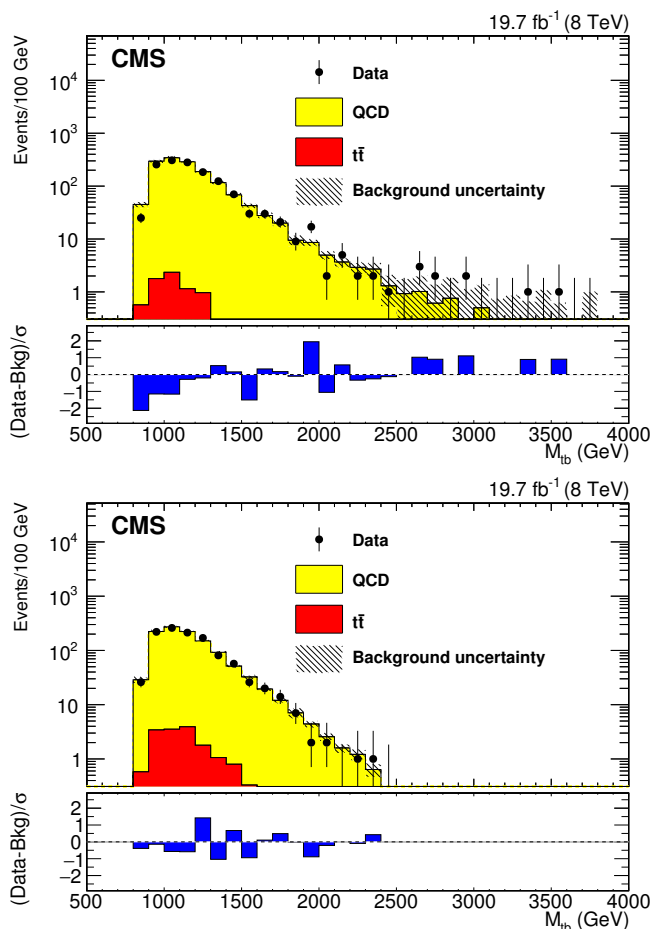
Figure 3. Distributions of M_{tb} shown for data, $\mathrm{t\bar{t}}$, and QCD in the control regions CR1 (top) and CR2 (bottom) as defined in the text. The hatched region shows the background uncertainty, obtained by adding the statistical and systematic uncertainties in quadrature. The bottom plots show the pull ((data-background)/σ) between the data and the background estimate distributions.

Control Region	Data	QCD	$\mathrm{t\bar{t}}$
CR1: $M_{\min} < 50\,\mathrm{GeV}$; $\tau_3/\tau_2 > 0.55$	1100	1107	15
CR2: $\mathrm{SJ_{CSVMAX}} < 0.679$	1376	1466	8
CR3: $M_{\mathrm{b}} > 70\,\mathrm{GeV}$	336	121	200

Table 2. Numbers of observed and expected events for each of the sidebands used for closure tests of the QCD and $\mathrm{t\bar{t}}$ background estimates. A summary of the inverted selection for each control region is provided.

6.1 Systematic uncertainties

We consider several sources of systematic uncertainty, corresponding to uncertainties in both the shape and normalization of the M_{tb} distribution, which are summarized in table 2.

A 19% normalization uncertainty is assigned to the estimate of the SM $\mathrm{t\bar{t}}$ normalization (see section 5.2). The scale factor used to account for differences in the t-tagging efficiency

between MC and data has an uncertainty of 13% [32]. The uncertainty in the integrated luminosity is 2.6% [41]. Finally, the MC to data scale factor for the b-tagging efficiency is evaluated using AK jets but is applied to CA jets, which requires a systematic uncertainty of 2% in addition to the b-tagging scale factor uncertainty of around 8%.

Several uncertainty sources contribute to the estimation of the average b-tagging rate, which is used to evaluate the QCD background prediction. We include a contribution due to the uncertainties obtained from the polynomial fit used to parameterize the b-tagging rate, and investigate the effect of choosing alternative functional forms in the fit. We also obtain an estimate of the uncertainty caused by the specific parameterization of the average b-tagging rate by studying an alternative parameterization using p_T, η, and M_tb.

We derive an uncertainty in the effect of p_T reweighting on the shape of the $t\bar{t}$ background by taking the unweighted M_tb distribution as the $+1\sigma$ shape.

The uncertainty arising from the variation of the renormalization and factorization scales in $t\bar{t}$ production is evaluated from MC samples generated with two times ($+1\sigma$) and one half (-1σ) the nominal renormalization and factorization scales.

The b-tagging scale factor $\pm1\sigma$ values are applied to $t\bar{t}$ production and signal MC [34]. The nominal jet energy corrections created for use with AK jets are applied in the analysis. The $\pm1\sigma$ uncertainties in jet energy scale and resolution arising from the application of AK jet energy scale corrections are also considered. Additionally, a 3% uncertainty is applied to the jet energy scale to account for differences in CA and AK jets. Finally, the uncertainty in the trigger turn-on efficiency that is applied to the MC samples is taken as one half of the trigger inefficiency.

Uncertainties arising from parton distribution functions are studied by varying the eigenvalues of the parton distribution functions that are used in the simulation. Pileup modeling in simulation is corrected by comparing the number of pileup interactions to the mean number of interactions in data. The uncertainty on this correction is studied by varying the minimum bias cross section. These sources, along with the jet angular resolution variation, are negligible.

The two largest systematic effects arise from the uncertainties in the average b-tagging rate for the QCD background (approximately a 6% normalization effect) and in the top tagging scale factor for the signal (13%).

6.2 Cross section limits

To set limits on the production cross section of the W'_R boson model described in eq. (1.1), we compare, for each bin in the M_tb distribution, the numbers of observed and expected events. The small background contribution from single top quark production is not considered when setting limits. The following expression is used to compute the expected contribution from W'_R boson production:

$$N_\mathrm{expected} = \sigma_{\mathrm{W}'_\mathrm{R}} \, \mathcal{B}_{\mathrm{W}'_\mathrm{R} \to \mathrm{tb}; \mathrm{W} \to \mathrm{hadrons}} \, \varepsilon \int L \, \mathrm{d}t, \qquad (6.1)$$

where $\sigma_{\mathrm{W}'_\mathrm{R}}$ is the W'_R cross section, $\mathcal{B}_{\mathrm{W}'_\mathrm{R} \to \mathrm{tb}; \mathrm{W} \to \mathrm{hadrons}}$ is the branching fraction $\mathrm{W}'_\mathrm{R} \to \mathrm{tb}$ with the W boson decay constrained to the hadronic branching fraction, ε is the signal
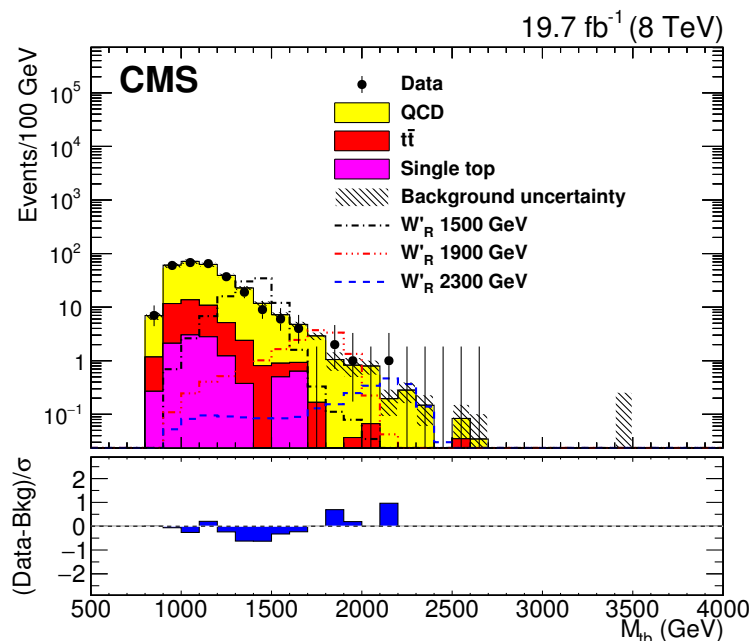
Figure 4. The distribution of M_{tb} shown for data, $t\bar{t}$, QCD, single top, and several example signal W' boson mass hypotheses. The normalization for the W' signal samples assumes the cross section from theory. The distributions are shown after the application of all selection criteria. The background contribution from single top quark production is not considered when setting limits. The hatched region shows the background uncertainty, obtained by adding the statistical and systematic uncertainties in quadrature. The bottom plot shows the pull ((data-background)/σ) between the data and the background estimate distributions.

Source	Variation
$t\bar{t}$ normalization	19%
t-tagging scale factor	13%
Integrated luminosity	2.6%
anti-k_T to CA8 jets b-tagging scale factor	2%
Average b-tagging rate fit	$\pm 1\sigma(p_T, \eta)$
Alternate functional forms for the average b-tagging rate	$\pm 1\sigma(p_T, \eta)$
Parameterization choice for the average b-tagging rate	$\pm 1\sigma(p_T, \eta, M_{tb})$
p_T reweighting	Shape $\pm 1\sigma(p_{T_t}, p_{T_{\bar{t}}})$
Renormalization and factorization scales	$2Q^2$ and $0.5Q^2$
b-tagging scale factor	$\pm 1\sigma(p_T)$
Jet energy scale	$\pm 1\sigma(p_T, \eta)$
Jet energy resolution	$\pm 1\sigma(\eta)$
Trigger efficiency	$\pm 1\sigma(p_{T1} + p_{T2})$

Table 3. Sources of uncertainty that affect the M_{tb} distribution and the $\pm 1\sigma$ variations that are used in the fit.

efficiency, and $\int L\,dt$ is the integrated luminosity of the data set. We perform a binned maximum likelihood fit to compare the M_{tb} distribution from data with the W_R' boson signal hypothesis, summed together with the SM distribution obtained from the background estimation procedure described in section 5.

A Poisson model is used for each bin of the M_{tb} distribution. The mean of the Poisson distribution for each bin is taken to be:

$$\mu_i = \sum_k \beta_k \, T_{k,i}, \tag{6.2}$$

where k includes both the signal and background models, β_k is the Poisson mean for process k, and $T_{k,i}$ represents the fraction of events expected for each process k in bin i.

The likelihood function is then:

$$L(\beta_k) = \prod_i^{N_{bins}} \frac{\mu_i^{N_i^{data}} e^{-\mu_i}}{(N_i^{data})!}, \tag{6.3}$$

where N_i^{data} is the number of events in data for bin i.

Using a Bayesian approach with a flat prior for the signal cross section, we obtain 95% confidence level (CL) upper limits on the production cross section of W_R'. Pseudo-experiments are used to derive the $\pm 1\sigma$ deviations in the expected limit. The systematic uncertainties described above are accounted for by nuisance parameters and the posterior probability is refitted for each pseudo-experiment. The cross section upper limits are shown in figure 5. We exclude a W_R' boson with a mass less than 2.02 TeV at 95% CL .

We combine the results from the hadronic and leptonic W' decay modes to enhance the sensitivity of the analysis to W' production and the measurement of the coupling strengths of the W' boson to quarks. The analysis of the leptonic channel excludes a W' mass below 2.05 TeV, and is described in ref. [6]. The all hadronic and leptonic channels have similar sensitivity in the high W' mass regime, which leads to a large increase in sensitivity in the combined result.

The hadronic channel probes W' signal generated from a mass of 1.3 to 3.1 TeV because of the sensitivity of the boosted top jet tagging techniques, whereas the leptonic channel probes W' masses from 0.8 to 3.0 TeV because of the higher sensitivity at low W' mass. Therefore, the region of combined sensitivity ranges from a W' mass of 1.3 to 3.0 TeV. Below this region, only the leptonic channel limits are quoted.

There are points within the region of combined sensitivity where the signal sample exists for the leptonic channel but not for the hadronic channel. These intermediate mass points are reproduced using ROOFIT [42] template morphing to interpolate the shape of the M_{tb} spectrum. The generator level selection on the p_T of the b quark for the left-handed and mixed-coupling W' samples is taken into account by interpolating the selection efficiency for the intermediate mass points.

We assume that the uncertainties in jet energy scale, jet energy resolution, b-tagging scale factors, and the total integrated luminosity are correlated between the two samples. All other systematic uncertainties are assumed to be uncorrelated. These include the
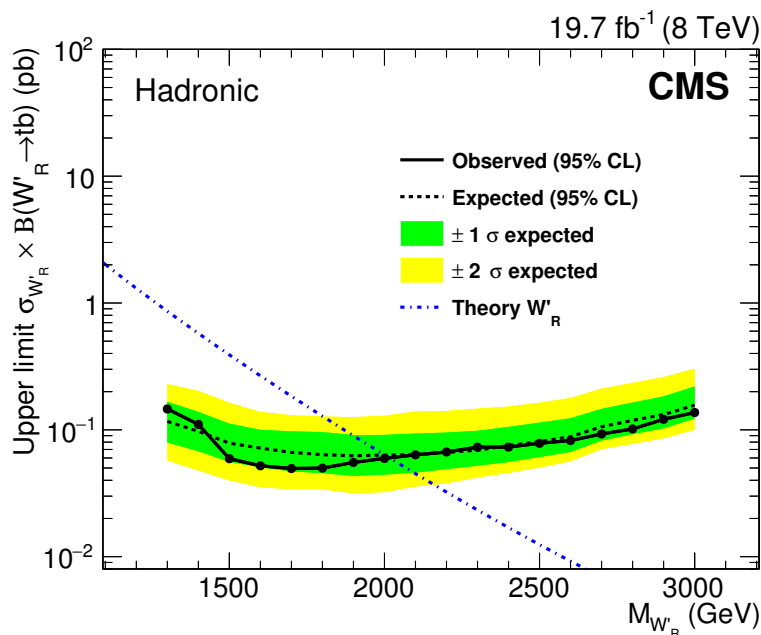
Figure 5. The W'_R boson 95% CL production cross section times $\mathcal{B}_{W'_R \to tb}$ limits for the hadronic channel. The observed (solid) and expected (dashed) limits, as well as the W'_R boson theoretical cross section (dot-dashed) are shown. As indicated in the legend, the shaded regions about the expected limits represent 1 and 2σ bands.

renormalization and factorization scale and p_T reweighting uncertainties, since different generators are used for the simulation of $t\bar{t}$ events and the hadronic channel extracts the $t\bar{t}$ normalization from data. The method for setting combined cross section upper limits is identical to the limit setting procedure of the all hadronic channel, except a joint likelihood is used that considers both channels.

The W'_R combined cross section upper limits are shown in figure 6. A W'_R boson with a mass below $2.15\,\text{TeV}$ is excluded at 95% CL.

6.3 Generalized coupling limits

To set limits on generic couplings, we use the procedure outlined in ref. [6]. Because the left-handed and mixed-coupling samples cannot be separated from SM single top quark production, we set limits on the couplings a^L and a^R. The SM single top quark production is negligible when setting cross section limits. As it is used for signal modeling in the generalized coupling analysis, it needs to be included in that calculation. For limit setting, we reweight the signal templates (single top quark, W'_R, W'_L, W'_{LR}) to form a combined signal template with the following cross section:

$$
\begin{aligned}
\sigma_{a^L_{ud},a^R_{ud},a^L_{tb},a^R_{tb}} = {} & \left(1 - a^L_{ud} a^L_{tb}\right)\sigma_t + a^R_{ud} a^R_{tb} \frac{a^R_{ud} a^R_{tb} - a^L_{ud} a^L_{tb}}{a^L_{ud} a^L_{tb} + a^R_{ud} a^R_{tb}}\sigma_{W'_R} \\
& + a^L_{ud} a^L_{tb} \frac{a^L_{ud} a^L_{tb} - a^R_{ud} a^R_{tb}}{a^L_{ud} a^L_{tb} + a^R_{ud} a^R_{tb}}\sigma_{W'_L} + 2\frac{a^R_{ud} a^R_{tb} a^L_{ud} a^L_{tb}}{a^L_{ud} a^L_{tb} + a^R_{ud} a^R_{tb}}\sigma_{W'_{LR}},
\end{aligned}
\tag{6.4}
$$

– 15 –
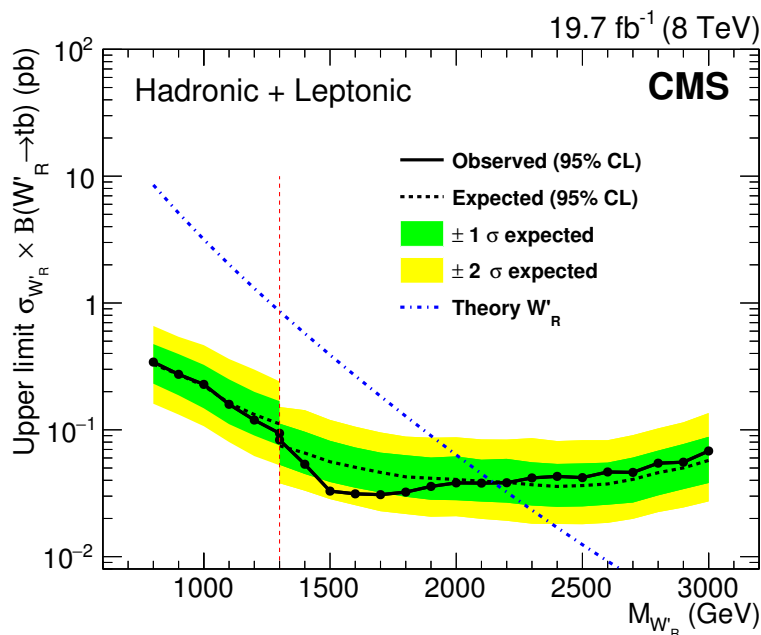
Figure 6. The W'_R boson 95% CL production cross section times $\mathcal{B}_{W'_R \to tb}$ limits for the combined hadronic and leptonic channels. The observed (solid) and expected (dashed) limits, as well as the W'_R boson theoretical cross section (dash-dotted) are shown. As indicated in the legend, the shaded regions about the expected limits represent 1 and 2σ bands. The region to the left of the vertical dashed line shows the limits derived only from the leptonic channel. The right of the vertical dashed line shows limits based on the combined hadronic and leptonic channels.

where $\sigma_{W'_R}$, $\sigma_{W'_L}$, $\sigma_{W'_{LR}}$ are the cross section for right-handed, left-handed, or mixed samples, respectively and σ_t is the SM s-channel single top quark production cross section. We assume that the left-handed and right-handed coupling constants are equal for first and third generation quarks ($a^L_{ud} = a^L_{tb}$ and $a^R_{ud} = a^R_{tb}$).

The templates are then summed and cross section upper limits are set using the resultant yield as the signal process for the given values of a^L and a^R. Limits are calculated using pairwise combinations of the couplings from 0 to 1 in increments of 0.1.

Using these cross section upper limits, we obtain the values where the $M_{W'}$ cross section limits are equal to the theoretical cross section prediction for a given combination of a^L and a^R. These points are the maximum excluded W' boson mass for given values of a^L and a^R. Exclusion limits when considering generalized couplings can therefore be represented with contours on a two dimensional plot in a^L and a^R and the contour is the maximum excluded W' boson mass. These contours in the (a^L, a^R) plane are shown in figure 7 for both observed and expected limits in the hadronic channel. The mass upper limits for left-handed and mixed-coupling W' bosons are 1.92 and 2.15 TeV, respectively.

For this procedure, no systematic uncertainty is considered from single top quark production since the templates are dominated by statistical uncertainties.

Additionally, we present combined limits on the W' coupling strengths, a^L and a^R. The limits for the leptonic channel that are used for the combination are shown in figure 8.
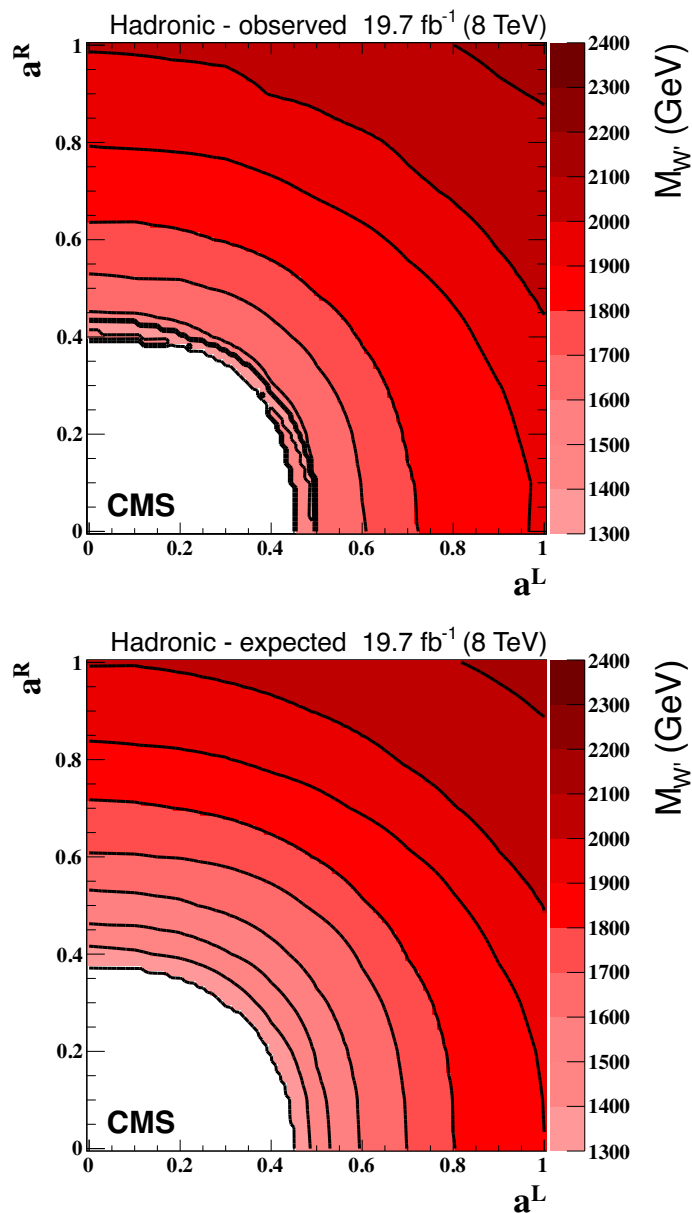
Figure 7. Contour plots of $M_{W'}$ in the (a^L, a^R) plane in the hadronic channel. The top (bottom) plot shows observed (expected) limits. The contour shading indicates the values of $M_{W'}$ where the theoretical cross section is equal to the observed or expected 95% CL limit.

These are updated from ref. [6] to include the effect of the W′ width on the cross section of an a^L and a^R combination. The limits for the combined hadronic and leptonic channels are shown in figure 9.

7 Summary

A search for a new massive gauge boson W′ decaying to a top and a bottom quark with a hadronic signature has been performed using proton-proton collisions recorded by the
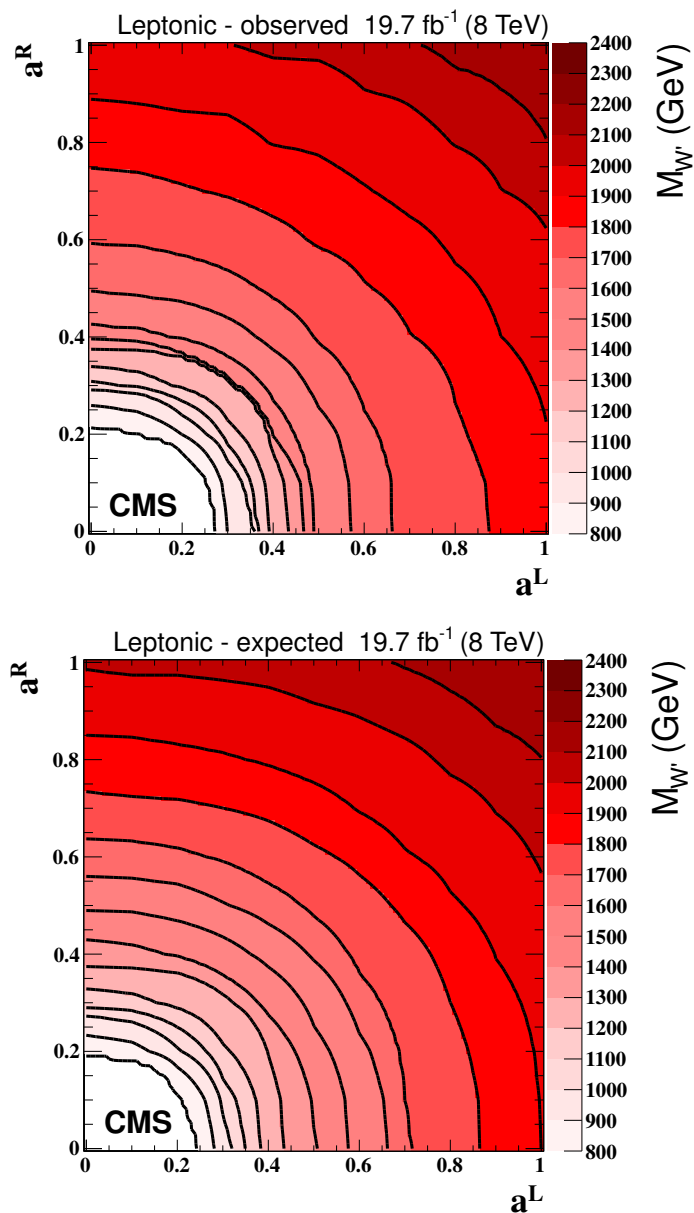
Figure 8. Contour plots of $M_{W'}$ in the (a^L, a^R) plane in the leptonic channel. The top (bottom) plot shows observed (expected) limits. The contour shading indicates the values of $M_{W'}$ where the theoretical cross section is equal to the observed or expected 95% CL limit. These are updated from ref. [6] to include the effect of the W' width on the cross section of an a^L and a^R combination.

CMS detector at $\sqrt{s} = 8\,\text{TeV}$, corresponding to an integrated luminosity of $19.7\,\text{fb}^{-1}$. The search is focused on W' masses above $1.30\,\text{TeV}$, where the main feature of this topology is a top quark whose decay products merge into a single jet.

The analysis uses jet substructure algorithms to distinguish the top quark jet from standard model hadronic jet backgrounds. The principal background, from QCD multijet
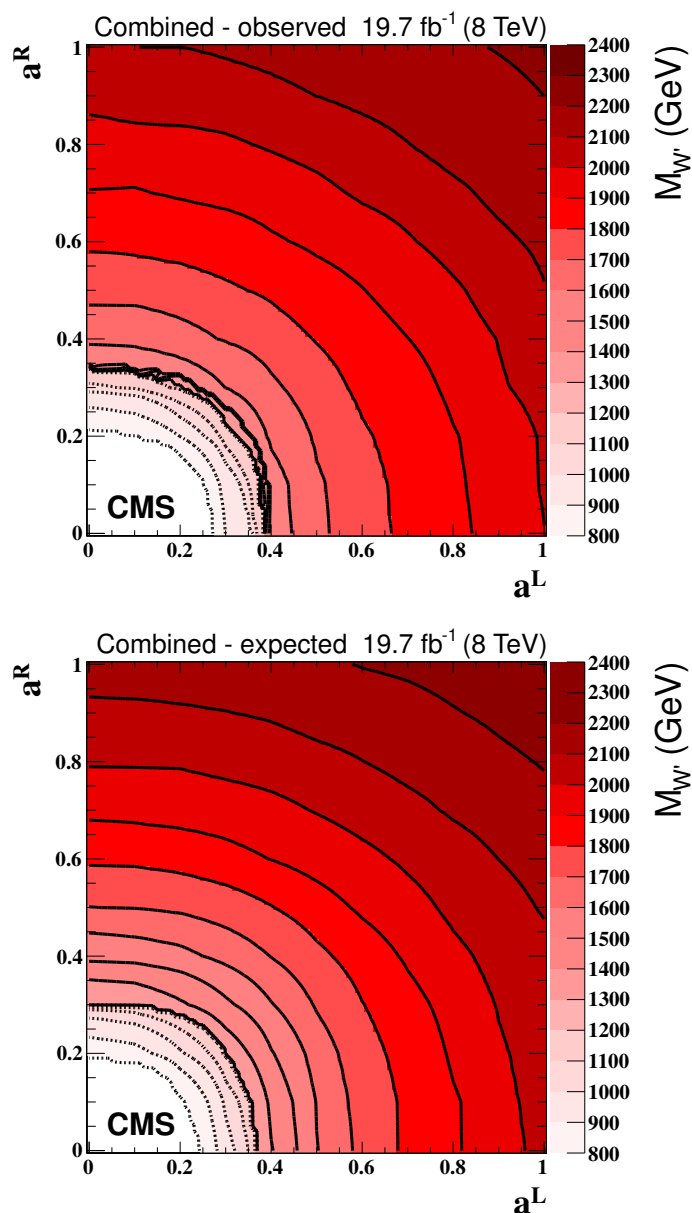
Figure 9. Contour plots of $M_{W'}$ in the $(a^L,\ a^R)$ plane using the combined hadronic and leptonic channels. The top (bottom) plot shows observed (expected) limits. The contour shading indicates the values of $M_{W'}$ where the theoretical cross section intersects the observed or expected limit band. The solid contours represent combined limits, and the dashed contours indicate limits that are obtained purely from the leptonic channel.

production, is estimated from data using the average b-tagging rate measured in a QCD enhanced control region. The other important source of background, from standard model $t\bar{t}$ production, is estimated from simulation, and is corrected by a scale factor derived from control samples in data.

Limits are placed on the production cross section of a right-handed W$'$ boson, together with constraints on the left-handed and right-handed couplings of the W$'$ boson to quarks.

The production of a right-handed W′ boson with a mass below 2.02 TeV decaying to a hadronic final state is excluded at 95% confidence level. The lower limit on the mass of the right-handed W′ boson increases to 2.15 TeV at 95% confidence level when both hadronic and leptonic decays are considered, and is the most stringent lower mass limit to date in the tb decay mode.

Acknowledgments

References

[1] M. Schmaltz and D. Tucker-Smith, *Little Higgs theoreis*, *Ann. Rev. Nucl. Part. Sci.* **55** (2005) 229 [hep-ph/0502182] [INSPIRE].

[2] T. Appelquist, H.-C. Cheng and B.A. Dobrescu, *Bounds on universal extra dimensions*, *Phys. Rev.* **D 64** (2001) 035002 [hep-ph/0012100] [INSPIRE].

[3] R.N. Mohapatra and J.C. Pati, *Left-right gauge symmetry and an isoconjugate model of CP-violation*, *Phys. Rev.* **D 11** (1975) 566 [INSPIRE].

[4] D0 collaboration, V.M. Abazov et al., *Search for W′ Boson Resonances Decaying to a Top Quark and a Bottom Quark*, *Phys. Rev. Lett.* **100** (2008) 211803 [arXiv:0803.3256] [INSPIRE].

[5] D0 collaboration, V.M. Abazov et al., *Search for W′ → tb resonances with left- and right-handed couplings to fermions*, *Phys. Lett.* **B 699** (2011) 145 [arXiv:1101.0806] [INSPIRE].

[6] CMS collaboration, *Search for W′ → tb decays in the lepton + jets final state in pp collisions at $\sqrt{s} = 8$ TeV*, *JHEP* **05** (2014) 108 [arXiv:1402.2176] [INSPIRE].

[7] CMS collaboration, *Search for physics beyond the standard model in final states with a lepton and missing transverse energy in proton-proton collisions at $\sqrt{s} = 8$ TeV*, *Phys. Rev.* **D 91** (2015) 092005 [arXiv:1408.2745] [INSPIRE].

[8] CMS collaboration, *Search for new resonances decaying via WZ to leptons in proton-proton collisions at $\sqrt{s} = 8$ TeV*, *Phys. Lett.* **B 740** (2015) 83 [arXiv:1407.3476] [INSPIRE].

[9] ATLAS collaboration, *ATLAS search for new phenomena in dijet mass and angular distributions using pp collisions at $\sqrt{s} = 7$ TeV*, *JHEP* **01** (2013) 029 [arXiv:1210.1718] [INSPIRE].

[10] ATLAS collaboration, *Search for resonant diboson production in the $WW/WZ \to \ell\nu jj$ decay channels with the ATLAS detector at $\sqrt{s} = 7$ TeV*, *Phys. Rev.* **D 87** (2013) 112006 [arXiv:1305.0125] [INSPIRE].

[11] ATLAS collaboration, *Search for $W' \to t\bar{b}$ in the lepton plus jets final state in proton-proton collisions at a centre-of-mass energy of $\sqrt{s} = 8$ TeV with the ATLAS detector*, *Phys. Lett.* **B 743** (2015) 235 [arXiv:1410.4103] [INSPIRE].

[12] ATLAS collaboration, *Search for $W' \to tb \to qqbb$ decays in pp collisions at $\sqrt{s} = 8$ TeV with the ATLAS detector*, *Eur. Phys. J.* **C 75** (2015) 165 [arXiv:1408.0886] [INSPIRE].

[13] ATLAS collaboration, *ATLAS search for a heavy gauge boson decaying to a charged lepton and a neutrino in pp collisions at $\sqrt{s} = 7$ TeV*, *Eur. Phys. J.* **C 72** (2012) 2241 [arXiv:1209.4446] [INSPIRE].

[14] CMS collaboration, *Search for massive resonances in dijet systems containing jets tagged as W or Z boson decays in pp collisions at $\sqrt{s} = 8$ TeV*, *JHEP* **08** (2014) 173 [arXiv:1405.1994] [INSPIRE].

[15] CMS collaboration, *Search for new physics in final states with a lepton and missing transverse energy in pp collisions at the LHC*, *Phys. Rev.* **D 87** (2013) 072005 [arXiv:1302.2812] [INSPIRE].

[16] D.J. Muller and S. Nandi, *Top flavor: a separate* SU(2) *for the third family*, *Phys. Lett.* **B 383** (1996) 345 [hep-ph/9602390] [INSPIRE].

[17] Z. Sullivan, *Fully differential W' production and decay at next-to-leading order in QCD*, *Phys. Rev.* **D 66** (2002) 075011 [hep-ph/0207290] [INSPIRE].

[18] CMS collaboration, *The CMS experiment at the CERN LHC*, 2008 *JINST* **3** S08004 [INSPIRE].

[19] CMS collaboration, *Description and performance of track and primary-vertex reconstruction with the CMS tracker*, 2014 *JINST* **9** P10009 [arXiv:1405.6569] [INSPIRE].

[20] CMS collaboration, *Particle-flow event reconstruction in CMS and performance for jets, taus and MET*, CMS-PAS-PFT-09-001 (2009).

[21] CMS collaboration, *Commissioning of the particle-flow event reconstruction with the first LHC collisions recorded in the CMS detector*, CMS-PAS-PFT-10-001 (2010).

[22] Y.L. Dokshitzer, G.D. Leder, S. Moretti and B.R. Webber, *Better jet clustering algorithms*, *JHEP* **08** (1997) 001 [hep-ph/9707323] [INSPIRE].

[23] M. Wobisch and T. Wengler, *Hadronization corrections to jet cross-sections in deep inelastic scattering*, hep-ph/9907280 [INSPIRE].

[24] M. Cacciari and G.P. Salam, *Dispelling the N^3 myth for the k_t jet-finder*, *Phys. Lett.* **B 641** (2006) 57 [hep-ph/0512210] [INSPIRE].

[25] M. Cacciari, G.P. Salam and G. Soyez, *FastJet user manual*, *Eur. Phys. J.* **C 72** (2012) 1896 [arXiv:1111.6097] [INSPIRE].

[26] CMS Collaboration, *A Cambridge-Aachen (C-A) based jet algorithm for boosted top-jet tagging*, CMS-PAS-JME-09-001 (2009).

[27] M. Cacciari, G.P. Salam and G. Soyez, *The anti-k_t jet clustering algorithm*, *JHEP* **04** (2008) 063 [arXiv:0802.1189] [INSPIRE].

[28] CMS collaboration, *Searches for new physics using the $t\bar{t}$ invariant mass distribution in pp collisions at $\sqrt{s} = 8$ TeV*, *Phys. Rev. Lett.* **111** (2013) 211804 [arXiv:1309.2030] [INSPIRE].

[29] CMS collaboration, *Pileup removal algorithms*, CMS-PAS-JME-14-001 (2014).

[30] M. Cacciari and G.P. Salam, *Pileup subtraction using jet areas*, *Phys. Lett.* **B 659** (2008) 119 [arXiv:0707.1378] [INSPIRE].

[31] CompHEP collaboration, E. Boos et al., *CompHEP 4.4: automatic computations from Lagrangians to events*, *Nucl. Instrum. Meth.* **A 534** (2004) 250 [hep-ph/0403113] [INSPIRE].

[32] CMS collaboration, *Boosted top jet tagging at CMS*, CMS-PAS-JME-13-007 (2013).

[33] J. Thaler and K. Van Tilburg, *Maximizing boosted top identification by minimizing N-subjettiness*, *JHEP* **02** (2012) 093 [arXiv:1108.2701] [INSPIRE].

[34] CMS collaboration, *Performance of b tagging at $\sqrt{s} = 8$ TeV in multijet, ttbar and boosted topology events*, CMS-PAS-BTV-13-001 (2013).

[35] S. Alioli, P. Nason, C. Oleari and E. Re, *A general framework for implementing NLO calculations in shower Monte Carlo programs: the POWHEG BOX*, *JHEP* **06** (2010) 043 [arXiv:1002.2581] [INSPIRE].

[36] S. Frixione, P. Nason and C. Oleari, *Matching NLO QCD computations with Parton Shower simulations: the POWHEG method*, *JHEP* **11** (2007) 070 [arXiv:0709.2092] [INSPIRE].

[37] P. Nason, *A New method for combining NLO QCD with shower Monte Carlo algorithms*, *JHEP* **11** (2004) 040 [hep-ph/0409146] [INSPIRE].

[38] M. Czakon, P. Fiedler and A. Mitov, *Total top-quark pair-production cross section at hadron colliders through $O(\alpha_S^4)$*, *Phys. Rev. Lett.* **110** (2013) 252004 [arXiv:1303.6254] [INSPIRE].

[39] N. Kidonakis, *Differential and total cross sections for top pair and single top production*, arXiv:1205.3453 [INSPIRE].

[40] CMS collaboration, *Measurement of differential top-quark pair production cross sections in the lepton+jets channel in pp collisions at 8 TeV*, CMS-PAS-TOP-12-027 (2012).

[41] CMS collaboration, *CMS luminosity based on pixel cluster counting — Summer 2013 update*, CMS-PAS-LUM-13-001 (2013).

[42] W. Verkerke and D.P. Kirkby, *The RooFit toolkit for data modeling*, *eConf* **C 0303241** (2003) MOLT007 [physics/0306116] [INSPIRE].

The CMS collaboration

Yerevan Physics Institute, Yerevan, Armenia

V. Khachatryan, A.M. Sirunyan, A. Tumasyan

Institut für Hochenergiephysik der OeAW, Wien, Austria

W. Adam, E. Asilar, T. Bergauer, J. Brandstetter, E. Brondolin, M. Dragicevic, J. Erö, M. Flechl, M. Friedl, R. Frühwirth[1], V.M. Ghete, C. Hartl, N. Hörmann, J. Hrubec, M. Jeitler[1], V. Knünz, A. König, M. Krammer[1], I. Krätschmer, D. Liko, I. Mikulec, D. Rabady[2], B. Rahbaran, H. Rohringer, J. Schieck[1], R. Schöfbeck, J. Strauss, W. Treberer-Treberspurg, W. Waltenberger, C.-E. Wulz[1]

National Centre for Particle and High Energy Physics, Minsk, Belarus

V. Mossolov, N. Shumeiko, J. Suarez Gonzalez

Universiteit Antwerpen, Antwerpen, Belgium

S. Alderweireldt, T. Cornelis, E.A. De Wolf, X. Janssen, A. Knutsson, J. Lauwers, S. Luyckx, S. Ochesanu, R. Rougny, M. Van De Klundert, H. Van Haevermaet, P. Van Mechelen, N. Van Remortel, A. Van Spilbeeck

Vrije Universiteit Brussel, Brussel, Belgium

S. Abu Zeid, F. Blekman, J. D'Hondt, N. Daci, I. De Bruyn, K. Deroover, N. Heracleous, J. Keaveney, S. Lowette, L. Moreels, A. Olbrechts, Q. Python, D. Strom, S. Tavernier, W. Van Doninck, P. Van Mulders, G.P. Van Onsem, I. Van Parijs

Université Libre de Bruxelles, Bruxelles, Belgium

P. Barria, C. Caillol, B. Clerbaux, G. De Lentdecker, H. Delannoy, D. Dobur, G. Fasanella, L. Favart, A.P.R. Gay, A. Grebenyuk, A. Léonard, A. Mohammadi, L. Perniè, A. Randle-conde, T. Reis, T. Seva, L. Thomas, C. Vander Velde, P. Vanlaer, J. Wang, F. Zenoni

Ghent University, Ghent, Belgium

K. Beernaert, L. Benucci, A. Cimmino, S. Crucy, A. Fagot, G. Garcia, M. Gul, J. Mccartin, A.A. Ocampo Rios, D. Poyraz, D. Ryckbosch, S. Salva, M. Sigamani, N. Strobbe, F. Thyssen, M. Tytgat, W. Van Driessche, E. Yazgan, N. Zaganidis

Université Catholique de Louvain, Louvain-la-Neuve, Belgium

S. Basegmez, C. Beluffi[3], O. Bondu, G. Bruno, R. Castello, A. Caudron, L. Ceard, G.G. Da Silveira, C. Delaere, T. du Pree, D. Favart, L. Forthomme, A. Giammanco[4], J. Hollar, A. Jafari, P. Jez, M. Komm, V. Lemaitre, A. Mertens, C. Nuttens, L. Perrini, A. Pin, K. Piotrzkowski, A. Popov[5], L. Quertenmont, M. Selvaggi, M. Vidal Marono

Université de Mons, Mons, Belgium

N. Beliy, T. Caebergs, G.H. Hammad

Centro Brasileiro de Pesquisas Fisicas, Rio de Janeiro, Brazil

W.L. Aldá Júnior, G.A. Alves, L. Brito, M. Correa Martins Junior, T. Dos Reis Martins, C. Hensel, C. Mora Herrera, A. Moraes, M.E. Pol, P. Rebello Teles

Universidade do Estado do Rio de Janeiro, Rio de Janeiro, Brazil

E. Belchior Batista Das Chagas, W. Carvalho, J. Chinellato[6], A. Custódio, E.M. Da Costa, D. De Jesus Damiao, C. De Oliveira Martins, S. Fonseca De Souza, L.M. Huertas Guativa, H. Malbouisson, D. Matos Figueiredo, L. Mundim, H. Nogima, W.L. Prado Da Silva, J. Santaolalla, A. Santoro, A. Sznajder, E.J. Tonelli Manganote[6], A. Vilela Pereira

Universidade Estadual Paulista [a], Universidade Federal do ABC [b], São Paulo, Brazil

S. Ahuja, C.A. Bernardes[b], S. Dogra[a], T.R. Fernandez Perez Tomei[a], E.M. Gregores[b], P.G. Mercadante[b], S.F. Novaes[a], Sandra S. Padula[a], D. Romero Abad, J.C. Ruiz Vargas

Institute for Nuclear Research and Nuclear Energy, Sofia, Bulgaria

A. Aleksandrov, V. Genchev[2], R. Hadjiiska, P. Iaydjiev, A. Marinov, S. Piperov, M. Rodozov, S. Stoykova, G. Sultanov, M. Vutova

University of Sofia, Sofia, Bulgaria

A. Dimitrov, I. Glushkov, L. Litov, B. Pavlov, P. Petkov

Institute of High Energy Physics, Beijing, China

M. Ahmad, J.G. Bian, G.M. Chen, H.S. Chen, M. Chen, T. Cheng, R. Du, C.H. Jiang, R. Plestina[7], F. Romeo, S.M. Shaheen, J. Tao, C. Wang, Z. Wang

State Key Laboratory of Nuclear Physics and Technology, Peking University, Beijing, China

C. Asawatangtrakuldee, Y. Ban, Q. Li, S. Liu, Y. Mao, S.J. Qian, D. Wang, Z. Xu, F. Zhang[8], L. Zhang, W. Zou

Universidad de Los Andes, Bogota, Colombia

C. Avila, A. Cabrera, L.F. Chaparro Sierra, C. Florez, J.P. Gomez, B. Gomez Moreno, J.C. Sanabria

University of Split, Faculty of Electrical Engineering, Mechanical Engineering and Naval Architecture, Split, Croatia

N. Godinovic, D. Lelas, D. Polic, I. Puljak

University of Split, Faculty of Science, Split, Croatia

Z. Antunovic, M. Kovac

Institute Rudjer Boskovic, Zagreb, Croatia

V. Brigljevic, K. Kadija, J. Luetic, L. Sudic

University of Cyprus, Nicosia, Cyprus

A. Attikis, G. Mavromanolakis, J. Mousa, C. Nicolaou, F. Ptochos, P.A. Razis, H. Rykaczewski

Charles University, Prague, Czech Republic

M. Bodlak, M. Finger, M. Finger Jr.[9]

Academy of Scientific Research and Technology of the Arab Republic of Egypt, Egyptian Network of High Energy Physics, Cairo, Egypt

R. Aly[10], S. Aly[10], Y. Assran[11], S. Elgammal[12], A. Ellithi Kamel[13], A. Lotfy[14], M.A. Mahmoud[14], A. Radi[12,15], A. Sayed[15,12]

National Institute of Chemical Physics and Biophysics, Tallinn, Estonia

B. Calpas, M. Kadastik, M. Murumaa, M. Raidal, A. Tiko, C. Veelken

Department of Physics, University of Helsinki, Helsinki, Finland

P. Eerola, M. Voutilainen

Helsinki Institute of Physics, Helsinki, Finland

J. Härkönen, V. Karimäki, R. Kinnunen, T. Lampén, K. Lassila-Perini, S. Lehti, T. Lindén, P. Luukka, T. Mäenpää, T. Peltola, E. Tuominen, J. Tuominiemi, E. Tuovinen, L. Wendland

Lappeenranta University of Technology, Lappeenranta, Finland

J. Talvitie, T. Tuuva

DSM/IRFU, CEA/Saclay, Gif-sur-Yvette, France

M. Besancon, F. Couderc, M. Dejardin, D. Denegri, B. Fabbro, J.L. Faure, C. Favaro, F. Ferri, S. Ganjour, A. Givernaud, P. Gras, G. Hamel de Monchenault, P. Jarry, E. Locci, J. Malcles, J. Rander, A. Rosowsky, M. Titov, A. Zghiche

Laboratoire Leprince-Ringuet, Ecole Polytechnique, IN2P3-CNRS, Palaiseau, France

S. Baffioni, F. Beaudette, P. Busson, L. Cadamuro, E. Chapon, C. Charlot, T. Dahms, O. Davignon, N. Filipovic, A. Florent, R. Granier de Cassagnac, L. Mastrolorenzo, P. Miné, I.N. Naranjo, M. Nguyen, C. Ochando, G. Ortona, P. Paganini, S. Regnard, R. Salerno, J.B. Sauvan, Y. Sirois, T. Strebler, Y. Yilmaz, A. Zabi

Institut Pluridisciplinaire Hubert Curien, Université de Strasbourg, Université de Haute Alsace Mulhouse, CNRS/IN2P3, Strasbourg, France

J.-L. Agram[16], J. Andrea, A. Aubin, D. Bloch, J.-M. Brom, M. Buttignol, E.C. Chabert, N. Chanon, C. Collard, E. Conte[16], J.-C. Fontaine[16], D. Gelé, U. Goerlach, C. Goetzmann, A.-C. Le Bihan, J.A. Merlin[2], K. Skovpen, P. Van Hove

Centre de Calcul de l'Institut National de Physique Nucleaire et de Physique des Particules, CNRS/IN2P3, Villeurbanne, France

S. Gadrat

Université de Lyon, Université Claude Bernard Lyon 1, CNRS-IN2P3, Institut de Physique Nucléaire de Lyon, Villeurbanne, France

S. Beauceron, N. Beaupere, C. Bernet[7], G. Boudoul[2], E. Bouvier, S. Brochet, C.A. Carrillo Montoya, J. Chasserat, R. Chierici, D. Contardo, B. Courbon, P. Depasse, H. El Mamouni, J. Fan, J. Fay, S. Gascon, M. Gouzevitch, B. Ille, I.B. Laktineh, M. Lethuillier, L. Mirabito, A.L. Pequegnot, S. Perries, J.D. Ruiz Alvarez, D. Sabes, L. Sgandurra, V. Sordini, M. Vander Donckt, P. Verdier, S. Viret, H. Xiao

Georgian Technical University, Tbilisi, Georgia

T. Toriashvili[17]

Tbilisi State University, Tbilisi, Georgia

Z. Tsamalaidze[9]

RWTH Aachen University, I. Physikalisches Institut, Aachen, Germany

C. Autermann, S. Beranek, M. Edelhoff, L. Feld, A. Heister, M.K. Kiesel, K. Klein, M. Lipinski, A. Ostapchuk, M. Preuten, F. Raupach, J. Sammet, S. Schael, J.F. Schulte, T. Verlage, H. Weber, B. Wittmer, V. Zhukov[5]

RWTH Aachen University, III. Physikalisches Institut A, Aachen, Germany

M. Ata, M. Brodski, E. Dietz-Laursonn, D. Duchardt, M. Endres, M. Erdmann, S. Erdweg, T. Esch, R. Fischer, A. Güth, T. Hebbeker, C. Heidemann, K. Hoepfner, D. Klingebiel, S. Knutzen, P. Kreuzer, M. Merschmeyer, A. Meyer, P. Millet, M. Olschewski, K. Padeken, P. Papacz, T. Pook, M. Radziej, H. Reithler, M. Rieger, S.A. Schmitz, L. Sonnenschein, D. Teyssier, S. Thüer

RWTH Aachen University, III. Physikalisches Institut B, Aachen, Germany

V. Cherepanov, Y. Erdogan, G. Flügge, H. Geenen, M. Geisler, W. Haj Ahmad, F. Hoehle, B. Kargoll, T. Kress, Y. Kuessel, A. Künsken, J. Lingemann[2], A. Nowack, I.M. Nugent, C. Pistone, O. Pooth, A. Stahl

Deutsches Elektronen-Synchrotron, Hamburg, Germany

M. Aldaya Martin, I. Asin, N. Bartosik, O. Behnke, U. Behrens, A.J. Bell, K. Borras, A. Burgmeier, A. Cakir, L. Calligaris, A. Campbell, S. Choudhury, F. Costanza, C. Diez Pardos, G. Dolinska, S. Dooling, T. Dorland, G. Eckerlin, D. Eckstein, T. Eichhorn, G. Flucke, J. Garay Garcia, A. Geiser, A. Gizhko, P. Gunnellini, J. Hauk, M. Hempel[18], H. Jung, A. Kalogeropoulos, O. Karacheban[18], M. Kasemann, P. Katsas, J. Kieseler, C. Kleinwort, I. Korol, W. Lange, J. Leonard, K. Lipka, A. Lobanov, R. Mankel, I. Marfin[18], I.-A. Melzer-Pellmann, A.B. Meyer, G. Mittag, J. Mnich, A. Mussgiller, S. Naumann-Emme, A. Nayak, E. Ntomari, H. Perrey, D. Pitzl, R. Placakyte, A. Raspereza, P.M. Ribeiro Cipriano, B. Roland, M.Ö. Sahin, J. Salfeld-Nebgen, P. Saxena, T. Schoerner-Sadenius, M. Schröder, C. Seitz, S. Spannagel, C. Wissing

University of Hamburg, Hamburg, Germany

V. Blobel, M. Centis Vignali, A.R. Draeger, J. Erfle, E. Garutti, K. Goebel, D. Gonzalez, M. Görner, J. Haller, M. Hoffmann, R.S. Höing, A. Junkes, H. Kirschenmann, R. Klanner, R. Kogler, T. Lapsien, T. Lenz, I. Marchesini, D. Marconi, D. Nowatschin, J. Ott, T. Peiffer, A. Perieanu, N. Pietsch, J. Poehlsen, D. Rathjens, C. Sander, H. Schettler, P. Schleper, E. Schlieckau, A. Schmidt, M. Seidel, V. Sola, H. Stadie, G. Steinbrück, H. Tholen, D. Troendle, E. Usai, L. Vanelderen, A. Vanhoefer

Institut für Experimentelle Kernphysik, Karlsruhe, Germany

M. Akbiyik, C. Barth, C. Baus, J. Berger, C. Böser, E. Butz, T. Chwalek, F. Colombo, W. De Boer, A. Descroix, A. Dierlamm, M. Feindt, F. Frensch, M. Giffels, A. Gilbert, F. Hartmann[2], U. Husemann, I. Katkov[5], A. Kornmayer[2], P. Lobelle Pardo, M.U. Mozer,

T. Müller, Th. Müller, M. Plagge, G. Quast, K. Rabbertz, S. Röcker, F. Roscher, H.J. Simonis, F.M. Stober, R. Ulrich, J. Wagner-Kuhr, S. Wayand, T. Weiler, C. Wöhrmann, R. Wolf

Institute of Nuclear and Particle Physics (INPP), NCSR Demokritos, Aghia Paraskevi, Greece
G. Anagnostou, G. Daskalakis, T. Geralis, V.A. Giakoumopoulou, A. Kyriakis, D. Loukas, A. Markou, A. Psallidas, I. Topsis-Giotis

University of Athens, Athens, Greece
A. Agapitos, S. Kesisoglou, A. Panagiotou, N. Saoulidou, E. Tziaferi

University of Ioánnina, Ioánnina, Greece
I. Evangelou, G. Flouris, C. Foudas, P. Kokkas, N. Loukas, N. Manthos, I. Papadopoulos, E. Paradas, J. Strologas

Wigner Research Centre for Physics, Budapest, Hungary
G. Bencze, C. Hajdu, A. Hazi, P. Hidas, D. Horvath[19], F. Sikler, V. Veszpremi, G. Vesztergombi[20], A.J. Zsigmond

Institute of Nuclear Research ATOMKI, Debrecen, Hungary
N. Beni, S. Czellar, J. Karancsi[21], J. Molnar, J. Palinkas, Z. Szillasi

University of Debrecen, Debrecen, Hungary
M. Bartók[22], A. Makovec, P. Raics, Z.L. Trocsanyi

National Institute of Science Education and Research, Bhubaneswar, India
P. Mal, K. Mandal, N. Sahoo, S.K. Swain

Panjab University, Chandigarh, India
S. Bansal, S.B. Beri, V. Bhatnagar, R. Chawla, R. Gupta, U.Bhawandeep, A.K. Kalsi, A. Kaur, M. Kaur, R. Kumar, A. Mehta, M. Mittal, N. Nishu, J.B. Singh, G. Walia

University of Delhi, Delhi, India
Ashok Kumar, Arun Kumar, A. Bhardwaj, B.C. Choudhary, A. Kumar, S. Malhotra, M. Naimuddin, K. Ranjan, R. Sharma, V. Sharma

Saha Institute of Nuclear Physics, Kolkata, India
S. Banerjee, S. Bhattacharya, K. Chatterjee, S. Dey, S. Dutta, B. Gomber, Sa. Jain, Sh. Jain, R. Khurana, N. Majumdar, A. Modak, K. Mondal, S. Mukherjee, S. Mukhopadhyay, A. Roy, D. Roy, S. Roy Chowdhury, S. Sarkar, M. Sharan

Bhabha Atomic Research Centre, Mumbai, India
A. Abdulsalam, D. Dutta, V. Jha, V. Kumar, A.K. Mohanty[2], L.M. Pant, P. Shukla, A. Topkar

Tata Institute of Fundamental Research, Mumbai, India
T. Aziz, S. Banerjee, S. Bhowmik[23], R.M. Chatterjee, R.K. Dewanjee, S. Dugad, S. Ganguly, S. Ghosh, M. Guchait, A. Gurtu[24], G. Kole, S. Kumar, M. Maity[23], G. Majumder, K. Mazumdar, G.B. Mohanty, B. Parida, K. Sudhakar, N. Sur, B. Sutar, N. Wickramage[25]

Indian Institute of Science Education and Research (IISER), Pune, India

S. Sharma

Institute for Research in Fundamental Sciences (IPM), Tehran, Iran

H. Bakhshiansohi, H. Behnamian, S.M. Etesami[26], A. Fahim[27], R. Goldouzian, M. Khakzad, M. Mohammadi Najafabadi, M. Naseri, S. Paktinat Mehdiabadi, F. Rezaei Hosseinabadi, B. Safarzadeh[28], M. Zeinali

University College Dublin, Dublin, Ireland

M. Felcini, M. Grunewald

INFN Sezione di Bari ^{a}**, Università di Bari** ^{b}**, Politecnico di Bari** ^{c}**, Bari, Italy**

M. Abbrescia^{a,b}, C. Calabria^{a,b}, C. Caputo^{a,b}, S.S. Chhibra^{a,b}, A. Colaleo^a, D. Creanza^{a,c}, L. Cristella^{a,b}, N. De Filippis^{a,c}, M. De Palma^{a,b}, L. Fiore^a, G. Iaselli^{a,c}, G. Maggi^{a,c}, M. Maggi^a, G. Miniello^{a,b}, S. My^{a,c}, S. Nuzzo^{a,b}, A. Pompili^{a,b}, G. Pugliese^{a,c}, R. Radogna^{a,b,2}, A. Ranieri^a, G. Selvaggi^{a,b}, A. Sharma^a, L. Silvestris^{a,2}, R. Venditti^{a,b}, P. Verwilligen^a

INFN Sezione di Bologna ^{a}**, Università di Bologna** ^{b}**, Bologna, Italy**

G. Abbiendi^a, C. Battilana, A.C. Benvenuti^a, D. Bonacorsi^{a,b}, S. Braibant-Giacomelli^{a,b}, L. Brigliadori^{a,b}, R. Campanini^{a,b}, P. Capiluppi^{a,b}, A. Castro^{a,b}, F.R. Cavallo^a, G. Codispoti^{a,b}, M. Cuffiani^{a,b}, G.M. Dallavalle^a, F. Fabbri^a, A. Fanfani^{a,b}, D. Fasanella^{a,b}, P. Giacomelli^a, C. Grandi^a, L. Guiducci^{a,b}, S. Marcellini^a, G. Masetti^a, A. Montanari^a, F.L. Navarria^{a,b}, A. Perrotta^a, A.M. Rossi^{a,b}, T. Rovelli^{a,b}, G.P. Siroli^{a,b}, N. Tosi^{a,b}, R. Travaglini^{a,b}

INFN Sezione di Catania ^{a}**, Università di Catania** ^{b}**, CSFNSM** ^{c}**, Catania, Italy**

G. Cappello^a, M. Chiorboli^{a,b}, S. Costa^{a,b}, F. Giordano^{a,2}, R. Potenza^{a,b}, A. Tricomi^{a,b}, C. Tuve^{a,b}

INFN Sezione di Firenze ^{a}**, Università di Firenze** ^{b}**, Firenze, Italy**

G. Barbagli^a, V. Ciulli^{a,b}, C. Civinini^a, R. D'Alessandro^{a,b}, E. Focardi^{a,b}, E. Gallo^a, S. Gonzi^{a,b}, V. Gori^{a,b}, P. Lenzi^{a,b}, M. Meschini^a, S. Paoletti^a, G. Sguazzoni^a, A. Tropiano^{a,b}, L. Viliani^{a,b}

INFN Laboratori Nazionali di Frascati, Frascati, Italy

L. Benussi, S. Bianco, F. Fabbri, D. Piccolo

INFN Sezione di Genova ^{a}**, Università di Genova** ^{b}**, Genova, Italy**

V. Calvelli^{a,b}, F. Ferro^a, M. Lo Vetere^{a,b}, E. Robutti^a, S. Tosi^{a,b}

INFN Sezione di Milano-Bicocca ^{a}**, Università di Milano-Bicocca** ^{b}**, Milano, Italy**

M.E. Dinardo^{a,b}, S. Fiorendi^{a,b}, S. Gennai^{a,2}, R. Gerosa^{a,b}, A. Ghezzi^{a,b}, P. Govoni^{a,b}, M.T. Lucchini^{a,b,2}, S. Malvezzi^a, R.A. Manzoni^{a,b}, B. Marzocchi^{a,b,2}, D. Menasce^a, L. Moroni^a, M. Paganoni^{a,b}, D. Pedrini^a, S. Ragazzi^{a,b}, N. Redaelli^a, T. Tabarelli de Fatis^{a,b}

INFN Sezione di Napoli ^{a}, Università di Napoli 'Federico II' ^{b}, Napoli, Italy, Università della Basilicata ^{c}, Potenza, Italy, Università G. Marconi ^{d}, Roma, Italy

S. Buontempo^a, N. Cavallo^{a,c}, S. Di Guida^{a,d,2}, M. Esposito^{a,b}, F. Fabozzi^{a,c}, A.O.M. Iorio^{a,b}, G. Lanza^a, L. Lista^a, S. Meola^{a,d,2}, M. Merola^a, P. Paolucci^{a,2}, C. Sciacca^{a,b}

INFN Sezione di Padova ^{a}, Università di Padova ^{b}, Padova, Italy, Università di Trento ^{c}, Trento, Italy

P. Azzi^{a,2}, N. Bacchetta^a, D. Bisello^{a,b}, A. Branca^{a,b}, R. Carlin^{a,b}, A. Carvalho Antunes De Oliveira^{a,b}, P. Checchia^a, M. Dall'Osso^{a,b}, T. Dorigo^a, F. Gasparini^{a,b}, U. Gasparini^{a,b}, A. Gozzelino^a, K. Kanishchev^{a,c}, S. Lacaprara^a, M. Margoni^{a,b}, A.T. Meneguzzo^{a,b}, J. Pazzini^{a,b}, N. Pozzobon^{a,b}, P. Ronchese^{a,b}, F. Simonetto^{a,b}, E. Torassa^a, M. Tosi^{a,b}, S. Ventura^a, M. Zanetti, P. Zotto^{a,b}, A. Zucchetta^{a,b}, G. Zumerle^{a,b}

INFN Sezione di Pavia ^{a}, Università di Pavia ^{b}, Pavia, Italy

M. Gabusi^{a,b}, A. Magnani^a, S.P. Ratti^{a,b}, V. Re^a, C. Riccardi^{a,b}, P. Salvini^a, I. Vai^a, P. Vitulo^{a,b}

INFN Sezione di Perugia ^{a}, Università di Perugia ^{b}, Perugia, Italy

L. Alunni Solestizi^{a,b}, M. Biasini^{a,b}, G.M. Bilei^a, D. Ciangottini^{a,b,2}, L. Fanò^{a,b}, P. Lariccia^{a,b}, G. Mantovani^{a,b}, M. Menichelli^a, A. Saha^a, A. Santocchia^{a,b}, A. Spiezia^{a,b,2}

INFN Sezione di Pisa ^{a}, Università di Pisa ^{b}, Scuola Normale Superiore di Pisa ^{c}, Pisa, Italy

K. Androsov^{a,29}, P. Azzurri^a, G. Bagliesi^a, J. Bernardini^a, T. Boccali^a, G. Broccolo^{a,c}, R. Castaldi^a, M.A. Ciocci^{a,29}, R. Dell'Orso^a, S. Donato^{a,c,2}, G. Fedi, F. Fiori^{a,c}, L. Foà^{a,c†}, A. Giassi^a, M.T. Grippo^{a,29}, F. Ligabue^{a,c}, T. Lomtadze^a, L. Martini^{a,b}, A. Messineo^{a,b}, C.S. Moon^{a,30}, F. Palla^a, A. Rizzi^{a,b}, A. Savoy-Navarro^{a,31}, A.T. Serban^a, P. Spagnolo^a, P. Squillacioti^{a,29}, R. Tenchini^a, G. Tonelli^{a,b}, A. Venturi^a, P.G. Verdini^a

INFN Sezione di Roma ^{a}, Università di Roma ^{b}, Roma, Italy

L. Barone^{a,b}, F. Cavallari^a, G. D'imperio^{a,b}, D. Del Re^{a,b}, M. Diemoz^a, S. Gelli^{a,b}, C. Jorda^a, E. Longo^{a,b}, F. Margaroli^{a,b}, P. Meridiani^a, F. Micheli^{a,b}, G. Organtini^{a,b}, R. Paramatti^a, F. Preiato^{a,b}, S. Rahatlou^{a,b}, C. Rovelli^a, F. Santanastasio^{a,b}, L. Soffi^{a,b}, P. Traczyk^{a,b,2}

INFN Sezione di Torino ^{a}, Università di Torino ^{b}, Torino, Italy, Università del Piemonte Orientale ^{c}, Novara, Italy

N. Amapane^{a,b}, R. Arcidiacono^{a,c}, S. Argiro^{a,b}, M. Arneodo^{a,c}, R. Bellan^{a,b}, C. Biino^a, N. Cartiglia^a, S. Casasso^{a,b}, M. Costa^{a,b}, R. Covarelli^{a,b}, P. De Remigis^a, A. Degano^{a,b}, G. Dellacasa^a, N. Demaria^a, L. Finco^{a,b,2}, C. Mariotti^a, S. Maselli^a, E. Migliore^{a,b}, V. Monaco^{a,b}, M. Musich^a, M.M. Obertino^{a,c}, L. Pacher^{a,b}, N. Pastrone^a, M. Pelliccioni^a, G.L. Pinna Angioni^{a,b}, A. Romero^{a,b}, M. Ruspa^{a,c}, R. Sacchi^{a,b}, A. Solano^{a,b}, A. Staiano^a

INFN Sezione di Trieste ^{a}, Università di Trieste ^{b}, Trieste, Italy

S. Belforte^a, V. Candelise^{a,b,2}, M. Casarsa^a, F. Cossutti^a, G. Della Ricca^{a,b}, B. Gobbo^a, C. La Licata^{a,b}, M. Marone^{a,b}, A. Schizzi^{a,b}, T. Umer^{a,b}, A. Zanetti^a

Kangwon National University, Chunchon, Korea

S. Chang, A. Kropivnitskaya, S.K. Nam

Kyungpook National University, Daegu, Korea

D.H. Kim, G.N. Kim, M.S. Kim, D.J. Kong, S. Lee, Y.D. Oh, H. Park, A. Sakharov, D.C. Son

Chonbuk National University, Jeonju, Korea

H. Kim, T.J. Kim, M.S. Ryu

Chonnam National University, Institute for Universe and Elementary Particles, Kwangju, Korea

S. Song

Korea University, Seoul, Korea

S. Choi, Y. Go, D. Gyun, B. Hong, M. Jo, H. Kim, Y. Kim, B. Lee, K. Lee, K.S. Lee, S. Lee, S.K. Park, Y. Roh

Seoul National University, Seoul, Korea

H.D. Yoo

University of Seoul, Seoul, Korea

M. Choi, J.H. Kim, J.S.H. Lee, I.C. Park, G. Ryu

Sungkyunkwan University, Suwon, Korea

Y. Choi, Y.K. Choi, J. Goh, D. Kim, E. Kwon, J. Lee, I. Yu

Vilnius University, Vilnius, Lithuania

A. Juodagalvis, J. Vaitkus

National Centre for Particle Physics, Universiti Malaya, Kuala Lumpur, Malaysia

Z.A. Ibrahim, J.R. Komaragiri, M.A.B. Md Ali^{32}, F. Mohamad Idris, W.A.T. Wan Abdullah

Centro de Investigacion y de Estudios Avanzados del IPN, Mexico City, Mexico

E. Casimiro Linares, H. Castilla-Valdez, E. De La Cruz-Burelo, I. Heredia-de La Cruz, A. Hernandez-Almada, R. Lopez-Fernandez, G. Ramirez Sanchez, A. Sanchez-Hernandez

Universidad Iberoamericana, Mexico City, Mexico

S. Carrillo Moreno, F. Vazquez Valencia

Benemerita Universidad Autonoma de Puebla, Puebla, Mexico

S. Carpinteyro, I. Pedraza, H.A. Salazar Ibarguen

Universidad Autónoma de San Luis Potosí, San Luis Potosí, Mexico

A. Morelos Pineda

University of Auckland, Auckland, New Zealand

D. Krofcheck

University of Canterbury, Christchurch, New Zealand

P.H. Butler, S. Reucroft

National Centre for Physics, Quaid-I-Azam University, Islamabad, Pakistan

A. Ahmad, M. Ahmad, Q. Hassan, H.R. Hoorani, W.A. Khan, T. Khurshid, M. Shoaib

National Centre for Nuclear Research, Swierk, Poland

H. Bialkowska, M. Bluj, B. Boimska, T. Frueboes, M. Górski, M. Kazana, K. Nawrocki, K. Romanowska-Rybinska, M. Szleper, P. Zalewski

Institute of Experimental Physics, Faculty of Physics, University of Warsaw, Warsaw, Poland

G. Brona, K. Bunkowski, K. Doroba, A. Kalinowski, M. Konecki, J. Krolikowski, M. Misiura, M. Olszewski, M. Walczak

Laboratório de Instrumentação e Física Experimental de Partículas, Lisboa, Portugal

P. Bargassa, C. Beirão Da Cruz E Silva, A. Di Francesco, P. Faccioli, P.G. Ferreira Parracho, M. Gallinaro, L. Lloret Iglesias, F. Nguyen, J. Rodrigues Antunes, J. Seixas, O. Toldaiev, D. Vadruccio, J. Varela, P. Vischia

Joint Institute for Nuclear Research, Dubna, Russia

S. Afanasiev, P. Bunin, M. Gavrilenko, I. Golutvin, I. Gorbunov, A. Kamenev, V. Karjavin, V. Konoplyanikov, A. Lanev, A. Malakhov, V. Matveev[33], P. Moisenz, V. Palichik, V. Perelygin, S. Shmatov, S. Shulha, N. Skatchkov, V. Smirnov, A. Zarubin

Petersburg Nuclear Physics Institute, Gatchina (St. Petersburg), Russia

V. Golovtsov, Y. Ivanov, V. Kim[34], E. Kuznetsova, P. Levchenko, V. Murzin, V. Oreshkin, I. Smirnov, V. Sulimov, L. Uvarov, S. Vavilov, A. Vorobyev

Institute for Nuclear Research, Moscow, Russia

Yu. Andreev, A. Dermenev, S. Gninenko, N. Golubev, A. Karneyeu, M. Kirsanov, N. Krasnikov, A. Pashenkov, D. Tlisov, A. Toropin

Institute for Theoretical and Experimental Physics, Moscow, Russia

V. Epshteyn, V. Gavrilov, N. Lychkovskaya, V. Popov, I. Pozdnyakov, G. Safronov, A. Spiridonov, E. Vlasov, A. Zhokin

National Research Nuclear University 'Moscow Engineering Physics Institute' (MEPhI), Moscow, Russia

A. Bylinkin

P.N. Lebedev Physical Institute, Moscow, Russia

V. Andreev, M. Azarkin[35], I. Dremin[35], M. Kirakosyan, A. Leonidov[35], G. Mesyats, S.V. Rusakov, A. Vinogradov

Skobeltsyn Institute of Nuclear Physics, Lomonosov Moscow State University, Moscow, Russia

A. Baskakov, A. Belyaev, E. Boos, M. Dubinin[36], L. Dudko, A. Ershov, A. Gribushin, V. Klyukhin, O. Kodolova, I. Lokhtin, I. Myagkov, S. Obraztsov, S. Petrushanko, V. Savrin, A. Snigirev

State Research Center of Russian Federation, Institute for High Energy Physics, Protvino, Russia

I. Azhgirey, I. Bayshev, S. Bitioukov, V. Kachanov, A. Kalinin, D. Konstantinov, V. Krychkine, V. Petrov, R. Ryutin, A. Sobol, L. Tourtchanovitch, S. Troshin, N. Tyurin, A. Uzunian, A. Volkov

University of Belgrade, Faculty of Physics and Vinca Institute of Nuclear Sciences, Belgrade, Serbia

P. Adzic[37], M. Ekmedzic, J. Milosevic, V. Rekovic

Centro de Investigaciones Energéticas Medioambientales y Tecnológicas (CIEMAT), Madrid, Spain

J. Alcaraz Maestre, E. Calvo, M. Cerrada, M. Chamizo Llatas, N. Colino, B. De La Cruz, A. Delgado Peris, D. Domínguez Vázquez, A. Escalante Del Valle, C. Fernandez Bedoya, J.P. Fernández Ramos, J. Flix, M.C. Fouz, P. Garcia-Abia, O. Gonzalez Lopez, S. Goy Lopez, J.M. Hernandez, M.I. Josa, E. Navarro De Martino, A. Pérez-Calero Yzquierdo, J. Puerta Pelayo, A. Quintario Olmeda, I. Redondo, L. Romero, M.S. Soares

Universidad Autónoma de Madrid, Madrid, Spain

C. Albajar, J.F. de Trocóniz, M. Missiroli, D. Moran

Universidad de Oviedo, Oviedo, Spain

H. Brun, J. Cuevas, J. Fernandez Menendez, S. Folgueras, I. Gonzalez Caballero, E. Palencia Cortezon, J.M. Vizan Garcia

Instituto de Física de Cantabria (IFCA), CSIC-Universidad de Cantabria, Santander, Spain

J.A. Brochero Cifuentes, I.J. Cabrillo, A. Calderon, J.R. Castiñeiras De Saa, J. Duarte Campderros, M. Fernandez, G. Gomez, A. Graziano, A. Lopez Virto, J. Marco, R. Marco, C. Martinez Rivero, F. Matorras, F.J. Munoz Sanchez, J. Piedra Gomez, T. Rodrigo, A.Y. Rodríguez-Marrero, A. Ruiz-Jimeno, L. Scodellaro, I. Vila, R. Vilar Cortabitarte

CERN, European Organization for Nuclear Research, Geneva, Switzerland

D. Abbaneo, E. Auffray, G. Auzinger, M. Bachtis, P. Baillon, A.H. Ball, D. Barney, A. Benaglia, J. Bendavid, L. Benhabib, J.F. Benitez, G.M. Berruti, G. Bianchi, P. Bloch, A. Bocci, A. Bonato, C. Botta, H. Breuker, T. Camporesi, G. Cerminara, S. Colafranceschi[38], M. D'Alfonso, D. d'Enterria, A. Dabrowski, V. Daponte, A. David, M. De Gruttola, F. De Guio, A. De Roeck, S. De Visscher, E. Di Marco, M. Dobson, M. Dordevic, N. Dupont, A. Elliott-Peisert, J. Eugster, G. Franzoni, W. Funk, D. Gigi, K. Gill, D. Giordano, M. Girone, F. Glege, R. Guida, S. Gundacker, M. Guthoff, J. Hammer, M. Hansen, P. Harris, J. Hegeman, V. Innocente, P. Janot, M.J. Kortelainen,

K. Kousouris, K. Krajczar, P. Lecoq, C. Lourenço, N. Magini, L. Malgeri, M. Mannelli, J. Marrouche, A. Martelli, L. Masetti, F. Meijers, S. Mersi, E. Meschi, F. Moortgat, S. Morovic, M. Mulders, M.V. Nemallapudi, H. Neugebauer, S. Orfanelli, L. Orsini, L. Pape, E. Perez, A. Petrilli, G. Petrucciani, A. Pfeiffer, D. Piparo, A. Racz, G. Rolandi[39], M. Rovere, M. Ruan, H. Sakulin, C. Schäfer, C. Schwick, A. Sharma, P. Silva, M. Simon, P. Sphicas[40], D. Spiga, J. Steggemann, B. Stieger, M. Stoye, Y. Takahashi, D. Treille, A. Tsirou, G.I. Veres[20], N. Wardle, H.K. Wöhri, A. Zagozdzinska[41], W.D. Zeuner

Paul Scherrer Institut, Villigen, Switzerland

W. Bertl, K. Deiters, W. Erdmann, R. Horisberger, Q. Ingram, H.C. Kaestli, D. Kotlinski, U. Langenegger, T. Rohe

Institute for Particle Physics, ETH Zurich, Zurich, Switzerland

F. Bachmair, L. Bäni, L. Bianchini, M.A. Buchmann, B. Casal, G. Dissertori, M. Dittmar, M. Donegà, M. Dünser, P. Eller, C. Grab, C. Heidegger, D. Hits, J. Hoss, G. Kasieczka, W. Lustermann, B. Mangano, A.C. Marini, M. Marionneau, P. Martinez Ruiz del Arbol, M. Masciovecchio, D. Meister, N. Mohr, P. Musella, F. Nessi-Tedaldi, F. Pandolfi, J. Pata, F. Pauss, L. Perrozzi, M. Peruzzi, M. Quittnat, M. Rossini, A. Starodumov[42], M. Takahashi, V.R. Tavolaro, K. Theofilatos, R. Wallny, H.A. Weber

Universität Zürich, Zurich, Switzerland

T.K. Aarrestad, C. Amsler[43], M.F. Canelli, V. Chiochia, A. De Cosa, C. Galloni, A. Hinzmann, T. Hreus, B. Kilminster, C. Lange, J. Ngadiuba, D. Pinna, P. Robmann, F.J. Ronga, D. Salerno, S. Taroni, Y. Yang

National Central University, Chung-Li, Taiwan

M. Cardaci, K.H. Chen, T.H. Doan, C. Ferro, M. Konyushikhin, C.M. Kuo, W. Lin, Y.J. Lu, R. Volpe, S.S. Yu

National Taiwan University (NTU), Taipei, Taiwan

R. Bartek, P. Chang, Y.H. Chang, Y.W. Chang, Y. Chao, K.F. Chen, P.H. Chen, C. Dietz, U. Grundler, W.-S. Hou, Y. Hsiung, Y.F. Liu, R.-S. Lu, M. Miñano Moya, E. Petrakou, J.F. Tsai, Y.M. Tzeng

Chulalongkorn University, Faculty of Science, Department of Physics, Bangkok, Thailand

B. Asavapibhop, G. Singh, N. Srimanobhas, N. Suwonjandee

Cukurova University, Adana, Turkey

A. Adiguzel, S. Cerci[44], C. Dozen, I. Dumanoglu, S. Girgis, G. Gokbulut, Y. Guler, E. Gurpinar, I. Hos, E.E. Kangal[45], A. Kayis Topaksu, G. Onengut[46], K. Ozdemir[47], S. Ozturk[48], B. Tali[44], H. Topakli[48], M. Vergili, C. Zorbilmez

Middle East Technical University, Physics Department, Ankara, Turkey

I.V. Akin, B. Bilin, S. Bilmis, B. Isildak[49], G. Karapinar[50], U.E. Surat, M. Yalvac, M. Zeyrek

Bogazici University, Istanbul, Turkey

E.A. Albayrak[51], E. Gülmez, M. Kaya[52], O. Kaya[53], T. Yetkin[54]

Istanbul Technical University, Istanbul, Turkey

K. Cankocak, Y.O. Günaydin[55], F.I. Vardarlı

Institute for Scintillation Materials of National Academy of Science of Ukraine, Kharkov, Ukraine

B. Grynyov

National Scientific Center, Kharkov Institute of Physics and Technology, Kharkov, Ukraine

L. Levchuk, P. Sorokin

University of Bristol, Bristol, United Kingdom

R. Aggleton, F. Ball, L. Beck, J.J. Brooke, E. Clement, D. Cussans, H. Flacher, J. Goldstein, M. Grimes, G.P. Heath, H.F. Heath, J. Jacob, L. Kreczko, C. Lucas, Z. Meng, D.M. Newbold[56], S. Paramesvaran, A. Poll, T. Sakuma, S. Seif El Nasr-storey, S. Senkin, D. Smith, V.J. Smith

Rutherford Appleton Laboratory, Didcot, United Kingdom

K.W. Bell, A. Belyaev[57], C. Brew, R.M. Brown, D.J.A. Cockerill, J.A. Coughlan, K. Harder, S. Harper, E. Olaiya, D. Petyt, C.H. Shepherd-Themistocleous, A. Thea, I.R. Tomalin, T. Williams, W.J. Womersley, S.D. Worm

Imperial College, London, United Kingdom

M. Baber, R. Bainbridge, O. Buchmuller, A. Bundock, D. Burton, M. Citron, D. Colling, L. Corpe, N. Cripps, P. Dauncey, G. Davies, A. De Wit, M. Della Negra, P. Dunne, A. Elwood, W. Ferguson, J. Fulcher, D. Futyan, G. Hall, G. Iles, G. Karapostoli, M. Kenzie, R. Lane, R. Lucas[56], L. Lyons, A.-M. Magnan, S. Malik, J. Nash, A. Nikitenko[42], J. Pela, M. Pesaresi, K. Petridis, D.M. Raymond, A. Richards, A. Rose, C. Seez, P. Sharp[†], A. Tapper, K. Uchida, M. Vazquez Acosta, T. Virdee, S.C. Zenz

Brunel University, Uxbridge, United Kingdom

J.E. Cole, P.R. Hobson, A. Khan, P. Kyberd, D. Leggat, D. Leslie, I.D. Reid, P. Symonds, L. Teodorescu, M. Turner

Baylor University, Waco, USA

J. Dittmann, K. Hatakeyama, A. Kasmi, H. Liu, N. Pastika, T. Scarborough

The University of Alabama, Tuscaloosa, USA

O. Charaf, S.I. Cooper, C. Henderson, P. Rumerio

Boston University, Boston, USA

A. Avetisyan, T. Bose, C. Fantasia, D. Gastler, P. Lawson, D. Rankin, C. Richardson, J. Rohlf, J. St. John, L. Sulak, D. Zou

Brown University, Providence, USA

J. Alimena, E. Berry, S. Bhattacharya, D. Cutts, Z. Demiragli, N. Dhingra, A. Ferapontov, A. Garabedian, U. Heintz, E. Laird, G. Landsberg, Z. Mao, M. Narain, S. Sagir, T. Sinthuprasith

University of California, Davis, Davis, USA

R. Breedon, G. Breto, M. Calderon De La Barca Sanchez, S. Chauhan, M. Chertok, J. Conway, R. Conway, P.T. Cox, R. Erbacher, M. Gardner, W. Ko, R. Lander, M. Mulhearn, D. Pellett, J. Pilot, F. Ricci-Tam, S. Shalhout, J. Smith, M. Squires, D. Stolp, M. Tripathi, S. Wilbur, R. Yohay

University of California, Los Angeles, USA

R. Cousins, P. Everaerts, C. Farrell, J. Hauser, M. Ignatenko, G. Rakness, D. Saltzberg, E. Takasugi, V. Valuev, M. Weber

University of California, Riverside, Riverside, USA

K. Burt, R. Clare, J. Ellison, J.W. Gary, G. Hanson, J. Heilman, M. Ivova PANEVA, P. Jandir, E. Kennedy, F. Lacroix, O.R. Long, A. Luthra, M. Malberti, M. Olmedo Negrete, A. Shrinivas, S. Sumowidagdo, H. Wei, S. Wimpenny

University of California, San Diego, La Jolla, USA

J.G. Branson, G.B. Cerati, S. Cittolin, R.T. D'Agnolo, A. Holzner, R. Kelley, D. Klein, D. Kovalskyi, J. Letts, I. Macneill, D. Olivito, S. Padhi, C. Palmer, M. Pieri, M. Sani, V. Sharma, S. Simon, M. Tadel, Y. Tu, A. Vartak, S. Wasserbaech[58], C. Welke, F. Würthwein, A. Yagil, G. Zevi Della Porta

University of California, Santa Barbara, Santa Barbara, USA

D. Barge, J. Bradmiller-Feld, C. Campagnari, A. Dishaw, V. Dutta, K. Flowers, M. Franco Sevilla, P. Geffert, C. George, F. Golf, L. Gouskos, J. Gran, J. Incandela, C. Justus, N. Mccoll, S.D. Mullin, J. Richman, D. Stuart, W. To, C. West, J. Yoo

California Institute of Technology, Pasadena, USA

D. Anderson, A. Apresyan, A. Bornheim, J. Bunn, Y. Chen, J. Duarte, A. Mott, H.B. Newman, C. Pena, M. Pierini, M. Spiropulu, J.R. Vlimant, S. Xie, R.Y. Zhu

Carnegie Mellon University, Pittsburgh, USA

V. Azzolini, A. Calamba, B. Carlson, T. Ferguson, Y. Iiyama, M. Paulini, J. Russ, M. Sun, H. Vogel, I. Vorobiev

University of Colorado Boulder, Boulder, USA

J.P. Cumalat, W.T. Ford, A. Gaz, F. Jensen, A. Johnson, M. Krohn, T. Mulholland, U. Nauenberg, J.G. Smith, K. Stenson, S.R. Wagner

Cornell University, Ithaca, USA

J. Alexander, A. Chatterjee, J. Chaves, J. Chu, S. Dittmer, N. Eggert, N. Mirman, G. Nicolas Kaufman, J.R. Patterson, A. Ryd, L. Skinnari, W. Sun, S.M. Tan, W.D. Teo, J. Thom, J. Thompson, J. Tucker, Y. Weng, P. Wittich

Fermi National Accelerator Laboratory, Batavia, USA

S. Abdullin, M. Albrow, J. Anderson, G. Apollinari, L.A.T. Bauerdick, A. Beretvas, J. Berryhill, P.C. Bhat, G. Bolla, K. Burkett, J.N. Butler, H.W.K. Cheung, F. Chlebana, S. Cihangir, V.D. Elvira, I. Fisk, J. Freeman, E. Gottschalk, L. Gray, D. Green, S. Grünendahl, O. Gutsche, J. Hanlon, D. Hare, R.M. Harris, J. Hirschauer, B. Hooberman, Z. Hu, S. Jindariani, M. Johnson, U. Joshi, A.W. Jung, B. Klima, B. Kreis, S. Kwan[†], S. Lammel, J. Linacre, D. Lincoln, R. Lipton, T. Liu, R. Lopes De Sá, J. Lykken, K. Maeshima, J.M. Marraffino, V.I. Martinez Outschoorn, S. Maruyama, D. Mason, P. McBride, P. Merkel, K. Mishra, S. Mrenna, S. Nahn, C. Newman-Holmes, V. O'Dell, O. Prokofyev, E. Sexton-Kennedy, A. Soha, W.J. Spalding, L. Spiegel, L. Taylor, S. Tkaczyk, N.V. Tran, L. Uplegger, E.W. Vaandering, C. Vernieri, M. Verzocchi, R. Vidal, A. Whitbeck, F. Yang, H. Yin

University of Florida, Gainesville, USA

D. Acosta, P. Avery, P. Bortignon, D. Bourilkov, A. Carnes, M. Carver, D. Curry, S. Das, G.P. Di Giovanni, R.D. Field, M. Fisher, I.K. Furic, J. Hugon, J. Konigsberg, A. Korytov, T. Kypreos, J.F. Low, P. Ma, K. Matchev, H. Mei, P. Milenovic[59], G. Mitselmakher, L. Muniz, D. Rank, A. Rinkevicius, L. Shchutska, M. Snowball, D. Sperka, S. Wang, J. Yelton

Florida International University, Miami, USA

S. Hewamanage, S. Linn, P. Markowitz, G. Martinez, J.L. Rodriguez

Florida State University, Tallahassee, USA

A. Ackert, J.R. Adams, T. Adams, A. Askew, J. Bochenek, B. Diamond, J. Haas, S. Hagopian, V. Hagopian, K.F. Johnson, A. Khatiwada, H. Prosper, V. Veeraraghavan, M. Weinberg

Florida Institute of Technology, Melbourne, USA

V. Bhopatkar, M. Hohlmann, H. Kalakhety, D. Mareskas-palcek, T. Roy, F. Yumiceva

University of Illinois at Chicago (UIC), Chicago, USA

M.R. Adams, L. Apanasevich, D. Berry, R.R. Betts, I. Bucinskaite, R. Cavanaugh, O. Evdokimov, L. Gauthier, C.E. Gerber, D.J. Hofman, P. Kurt, C. O'Brien, I.D. Sandoval Gonzalez, C. Silkworth, P. Turner, N. Varelas, Z. Wu, M. Zakaria

The University of Iowa, Iowa City, USA

B. Bilki[60], W. Clarida, K. Dilsiz, R.P. Gandrajula, M. Haytmyradov, V. Khristenko, J.-P. Merlo, H. Mermerkaya[61], A. Mestvirishvili, A. Moeller, J. Nachtman, H. Ogul, Y. Onel, F. Ozok[51], A. Penzo, S. Sen, C. Snyder, P. Tan, E. Tiras, J. Wetzel, K. Yi

Johns Hopkins University, Baltimore, USA

I. Anderson, B.A. Barnett, B. Blumenfeld, D. Fehling, L. Feng, A.V. Gritsan, P. Maksimovic, C. Martin, K. Nash, M. Osherson, M. Swartz, M. Xiao, Y. Xin

The University of Kansas, Lawrence, USA

P. Baringer, A. Bean, G. Benelli, C. Bruner, J. Gray, R.P. Kenny III, D. Majumder, M. Malek, M. Murray, D. Noonan, S. Sanders, R. Stringer, Q. Wang, J.S. Wood

Kansas State University, Manhattan, USA

I. Chakaberia, A. Ivanov, K. Kaadze, S. Khalil, M. Makouski, Y. Maravin, L.K. Saini, N. Skhirtladze, I. Svintradze

Lawrence Livermore National Laboratory, Livermore, USA

D. Lange, F. Rebassoo, D. Wright

University of Maryland, College Park, USA

C. Anelli, A. Baden, O. Baron, A. Belloni, B. Calvert, S.C. Eno, J.A. Gomez, N.J. Hadley, S. Jabeen, R.G. Kellogg, T. Kolberg, Y. Lu, A.C. Mignerey, K. Pedro, Y.H. Shin, A. Skuja, M.B. Tonjes, S.C. Tonwar

Massachusetts Institute of Technology, Cambridge, USA

A. Apyan, R. Barbieri, A. Baty, K. Bierwagen, S. Brandt, W. Busza, I.A. Cali, L. Di Matteo, G. Gomez Ceballos, M. Goncharov, D. Gulhan, M. Klute, Y.S. Lai, Y.-J. Lee, A. Levin, P.D. Luckey, C. Mcginn, X. Niu, C. Paus, D. Ralph, C. Roland, G. Roland, G.S.F. Stephans, K. Sumorok, M. Varma, D. Velicanu, J. Veverka, J. Wang, T.W. Wang, B. Wyslouch, M. Yang, V. Zhukova

University of Minnesota, Minneapolis, USA

B. Dahmes, A. Finkel, A. Gude, S.C. Kao, K. Klapoetke, Y. Kubota, J. Mans, S. Nourbakhsh, R. Rusack, N. Tambe, J. Turkewitz

University of Mississippi, Oxford, USA

J.G. Acosta, S. Oliveros

University of Nebraska-Lincoln, Lincoln, USA

E. Avdeeva, K. Bloom, S. Bose, D.R. Claes, A. Dominguez, C. Fangmeier, R. Gonzalez Suarez, R. Kamalieddin, J. Keller, D. Knowlton, I. Kravchenko, J. Lazo-Flores, F. Meier, J. Monroy, F. Ratnikov, J.E. Siado, G.R. Snow

State University of New York at Buffalo, Buffalo, USA

M. Alyari, J. Dolen, J. George, A. Godshalk, I. Iashvili, J. Kaisen, A. Kharchilava, A. Kumar, S. Rappoccio

Northeastern University, Boston, USA

G. Alverson, E. Barberis, D. Baumgartel, M. Chasco, A. Hortiangtham, A. Massironi, D.M. Morse, D. Nash, T. Orimoto, R. Teixeira De Lima, D. Trocino, R.-J. Wang, D. Wood, J. Zhang

Northwestern University, Evanston, USA

K.A. Hahn, A. Kubik, N. Mucia, N. Odell, B. Pollack, A. Pozdnyakov, M. Schmitt, S. Stoynev, K. Sung, M. Trovato, M. Velasco, S. Won

University of Notre Dame, Notre Dame, USA

A. Brinkerhoff, N. Dev, M. Hildreth, C. Jessop, D.J. Karmgard, N. Kellams, K. Lannon, S. Lynch, N. Marinelli, F. Meng, C. Mueller, Y. Musienko[33], T. Pearson, M. Planer, R. Ruchti, G. Smith, N. Valls, M. Wayne, M. Wolf, A. Woodard

The Ohio State University, Columbus, USA

L. Antonelli, J. Brinson, B. Bylsma, L.S. Durkin, S. Flowers, A. Hart, C. Hill, R. Hughes, K. Kotov, T.Y. Ling, B. Liu, W. Luo, D. Puigh, M. Rodenburg, B.L. Winer, H.W. Wulsin

Princeton University, Princeton, USA

O. Driga, P. Elmer, J. Hardenbrook, P. Hebda, S.A. Koay, P. Lujan, D. Marlow, T. Medvedeva, M. Mooney, J. Olsen, P. Piroué, X. Quan, H. Saka, D. Stickland, C. Tully, J.S. Werner, A. Zuranski

University of Puerto Rico, Mayaguez, USA

S. Malik

Purdue University, West Lafayette, USA

V.E. Barnes, D. Benedetti, D. Bortoletto, L. Gutay, M.K. Jha, M. Jones, K. Jung, M. Kress, N. Leonardo, D.H. Miller, N. Neumeister, F. Primavera, B.C. Radburn-Smith, X. Shi, I. Shipsey, D. Silvers, J. Sun, A. Svyatkovskiy, F. Wang, W. Xie, L. Xu, J. Zablocki

Purdue University Calumet, Hammond, USA

N. Parashar, J. Stupak

Rice University, Houston, USA

A. Adair, B. Akgun, Z. Chen, K.M. Ecklund, F.J.M. Geurts, W. Li, B. Michlin, M. Northup, B.P. Padley, R. Redjimi, J. Roberts, J. Rorie, Z. Tu, J. Zabel

University of Rochester, Rochester, USA

B. Betchart, A. Bodek, P. de Barbaro, R. Demina, Y. Eshaq, T. Ferbel, M. Galanti, A. Garcia-Bellido, P. Goldenzweig, J. Han, A. Harel, O. Hindrichs, A. Khukhunaishvili, G. Petrillo, M. Verzetti, D. Vishnevskiy

The Rockefeller University, New York, USA

L. Demortier

Rutgers, The State University of New Jersey, Piscataway, USA

S. Arora, A. Barker, J.P. Chou, C. Contreras-Campana, E. Contreras-Campana, D. Duggan, D. Ferencek, Y. Gershtein, R. Gray, E. Halkiadakis, D. Hidas, E. Hughes, S. Kaplan, R. Kunnawalkam Elayavalli, A. Lath, S. Panwalkar, M. Park, S. Salur, S. Schnetzer, D. Sheffield, S. Somalwar, R. Stone, S. Thomas, P. Thomassen, M. Walker

University of Tennessee, Knoxville, USA

M. Foerster, K. Rose, S. Spanier, A. York

Texas A&M University, College Station, USA

O. Bouhali[62], A. Castaneda Hernandez, M. Dalchenko, M. De Mattia, A. Delgado, S. Dildick, R. Eusebi, W. Flanagan, J. Gilmore, T. Kamon[63], V. Krutelyov, R. Montalvo, R. Mueller, I. Osipenkov, Y. Pakhotin, R. Patel, A. Perloff, J. Roe, A. Rose, A. Safonov, I. Suarez, A. Tatarinov, K.A. Ulmer

Texas Tech University, Lubbock, USA

N. Akchurin, C. Cowden, J. Damgov, C. Dragoiu, P.R. Dudero, J. Faulkner, K. Kovitanggoon, S. Kunori, K. Lamichhane, S.W. Lee, T. Libeiro, S. Undleeb, I. Volobouev

Vanderbilt University, Nashville, USA

E. Appelt, A.G. Delannoy, S. Greene, A. Gurrola, R. Janjam, W. Johns, C. Maguire, Y. Mao, A. Melo, P. Sheldon, B. Snook, S. Tuo, J. Velkovska, Q. Xu

University of Virginia, Charlottesville, USA

M.W. Arenton, S. Boutle, B. Cox, B. Francis, J. Goodell, R. Hirosky, A. Ledovskoy, H. Li, C. Lin, C. Neu, E. Wolfe, J. Wood, F. Xia

Wayne State University, Detroit, USA

C. Clarke, R. Harr, P.E. Karchin, C. Kottachchi Kankanamge Don, P. Lamichhane, J. Sturdy

University of Wisconsin, Madison, USA

D.A. Belknap, D. Carlsmith, M. Cepeda, A. Christian, S. Dasu, L. Dodd, S. Duric, E. Friis, M. Grothe, R. Hall-Wilton, M. Herndon, A. Hervé, P. Klabbers, A. Lanaro, A. Levine, K. Long, R. Loveless, A. Mohapatra, I. Ojalvo, T. Perry, G.A. Pierro, G. Polese, I. Ross, T. Ruggles, T. Sarangi, A. Savin, N. Smith, W.H. Smith, D. Taylor, N. Woods

22: Also at Wigner Research Centre for Physics, Budapest, Hungary

23: Also at University of Visva-Bharati, Santiniketan, India

24: Now at King Abdulaziz University, Jeddah, Saudi Arabia

25: Also at University of Ruhuna, Matara, Sri Lanka

26: Also at Isfahan University of Technology, Isfahan, Iran

27: Also at University of Tehran, Department of Engineering Science, Tehran, Iran

28: Also at Plasma Physics Research Center, Science and Research Branch, Islamic Azad University, Tehran, Iran

29: Also at Università degli Studi di Siena, Siena, Italy

30: Also at Centre National de la Recherche Scientifique (CNRS) - IN2P3, Paris, France

31: Also at Purdue University, West Lafayette, USA

32: Also at International Islamic University of Malaysia, Kuala Lumpur, Malaysia

33: Also at Institute for Nuclear Research, Moscow, Russia

34: Also at St. Petersburg State Polytechnical University, St. Petersburg, Russia

35: Also at National Research Nuclear University 'Moscow Engineering Physics Institute' (MEPhI), Moscow, Russia

36: Also at California Institute of Technology, Pasadena, USA

37: Also at Faculty of Physics, University of Belgrade, Belgrade, Serbia

38: Also at Facoltà Ingegneria, Università di Roma, Roma, Italy

39: Also at Scuola Normale e Sezione dell'INFN, Pisa, Italy

40: Also at University of Athens, Athens, Greece

41: Also at Warsaw University of Technology, Institute of Electronic Systems, Warsaw, Poland

42: Also at Institute for Theoretical and Experimental Physics, Moscow, Russia

43: Also at Albert Einstein Center for Fundamental Physics, Bern, Switzerland

44: Also at Adiyaman University, Adiyaman, Turkey

45: Also at Mersin University, Mersin, Turkey

46: Also at Cag University, Mersin, Turkey

47: Also at Piri Reis University, Istanbul, Turkey

48: Also at Gaziosmanpasa University, Tokat, Turkey

49: Also at Ozyegin University, Istanbul, Turkey

50: Also at Izmir Institute of Technology, Izmir, Turkey

51: Also at Mimar Sinan University, Istanbul, Istanbul, Turkey

52: Also at Marmara University, Istanbul, Turkey

53: Also at Kafkas University, Kars, Turkey

54: Also at Yildiz Technical University, Istanbul, Turkey

55: Also at Kahramanmaras Sütcü Imam University, Kahramanmaras, Turkey

56: Also at Rutherford Appleton Laboratory, Didcot, United Kingdom

57: Also at School of Physics and Astronomy, University of Southampton, Southampton, United Kingdom

58: Also at Utah Valley University, Orem, USA

59: Also at University of Belgrade, Faculty of Physics and Vinca Institute of Nuclear Sciences, Belgrade, Serbia

60: Also at Argonne National Laboratory, Argonne, USA

61: Also at Erzincan University, Erzincan, Turkey

62: Also at Texas A&M University at Qatar, Doha, Qatar

63: Also at Kyungpook National University, Daegu, Korea